Biomaterials Science

ROYAL SOCIETY OF CHEMISTRY

REVIEW

View Article Online
View Journal | View Issue

Cite this: *Biomater. Sci.*, 2026, **14**, 661

Advances in phenylboronic acid and phenylboronic ester-based responsive systems for precision medicine

Ratish R. Nair, Loise Råberg, Hanna Mårtensson, Fan Jia, Yifan Gu, Hamza Yakubu, Gizem Erensoy and Alexandra Stubelius *

Phenylboronic acid (PBA) and its ester derivates (PBE) are considered adaptable building blocks for smart biomaterials, enabling precision in therapeutic and diagnostic applications. Their reversible covalent interactions with *cis*-diols allow selective recognition of clinically relevant biomarkers including glucose, reactive oxygen species (ROS), and sialic acid (Sia). These properties have been exploited to engineer responsive systems for glucose-triggered insulin and glucagon delivery, ROS-mediated drug release in oxidative microenvironments, and Sia-targeted cancer therapies. Recent advances integrate PBA/PBE chemistries into multi-responsive platforms, closed-loop devices, and biosensors for real-time monitoring, making these materials key enablers of personalized treatment strategies. Here, we review design principles that govern binding specificity, summarize applications across a wide range of therapies, and discuss key challenges such as off-target interactions and physiological stability. Finally, we outline opportunities for clinical translation, positioning PBA/PBE-based materials as promising candidates for next generation precision medicines.

Received 7th November 2025,
Accepted 29th November 2025

DOI: 10.1039/d5bm01624j

rsc.li/biomaterials-science

1. Introduction

The development of biomaterials that respond to disease-specific biochemical cues is central to advancing personalized medicine. Among highly promising molecular tools in this domain are phenylboronic acid (PBA) and its ester derivatives (PBE) which form reversible covalent bonds with *cis*-diols, enabling selective interactions with biologically relevant molecules such as glucose, reactive oxygen species (ROS), and sialic acids (Sia). Their chemical structures, featuring a boron atom with a vacant p-orbital, allow dynamic Lewis acid–base interactions with oxygen and nitrogen nucleophiles, tunable by pH, solvent polarity, or diol stereochemistry.[1–3] These properties make PBA and PBE ideal components in smart biomaterials designed for real-time responsiveness and adaptive therapeutic

Division of Chemical Biology, Department of Life Sciences, Chalmers University of Technology, Gothenburg 412 96, Sweden. E-mail: alexandra.stubelius@chalmers.se

Ratish R. Nair

Ratish R. Nair received his Ph.D degree from AcSIR, CSIR-CSMCRI, Bhavnagar, Gujarat, India in 2020. He then worked as a postdoctoral fellow at Daegu university, South Korea till 2022. He then worked as a research professor at Kyunghee University, South Korea till 2024. Currently he is working as a postdoctoral fellow in the group of Associate Professor Alexandra Stubelius at Chalmers University of Technology. His research focuses on the development of diagnostic and therapeutic materials targeting infection and inflammation.

Loise Råberg

Loise Råberg earned her master's degree in molecular biology, specializing in medical biology, from Lund University in 2021. She is currently pursuing a PhD in the group of Associate Professor Alexandra Stubelius at Chalmers University of Technology. Her research focuses on the role of the monosaccharide sialic acid in osteoarthritis.

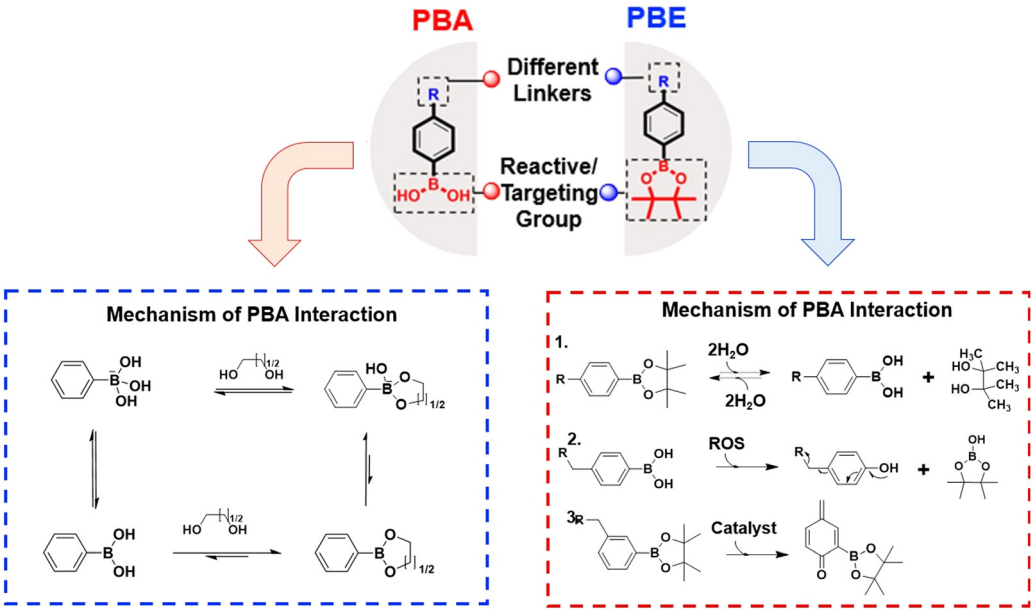

Fig. 1 Schematic representation of different interaction mechanisms involved with phenylboronic acids (PBA) and phenylboronic ester (PBE).

control. PBA's rapid and reversible binding to *cis*-diols under physiological conditions has enabled its use in glucose-responsive insulin delivery systems for diabetes, sialic acid-targeted cancer therapies, and biosensors for dynamic diseases monitoring.[4–12] PBE, formed *via* esterification with diols like pinacol, offers enhanced oxidative sensitivity and hydrolytic stability, making it particularly suitable for ROS triggered drug release in inflammatory and tumor microenvironments.[13]

The focus in this review is on glucose, ROS and Sia to reflect their relevance as clinically actionable biomarkers. Glucose levels fluctuate in metabolic disorders such as diabetes, demanding chronic therapeutic use, making it a key target for closed-loop drug delivery systems. ROS are elevated in several oxidative-stress related conditions including cancer, cardiovascular diseases and neurodegeneration, offering a trigger for site-specific therapeutic activation. Sia is emerging as a clinical target in several cancerous and immune-regulatory conditions, as it is often over expressed or dysregulated on glycoproteins, providing a unique glycan signature for targeted delivery and immunomodulation. By leveraging these biomarker-specific interactions, PBA/PBE-based materials enable personalized treatment strategies that adapt to individual pathophysiology. PBA's ability to form cyclic esters with *cis*-diols at high reaction rates (10^2–10^3 M^{-1} s^{-1}) under aqueous conditions underpins its utility in carbohydrate sensing, glycan targeting, and surface targeting.[14,15] The pK_a-shifting behavior upon sugar binding, first quantified by Edwards *et al.* in 1959,[16] provides a quantifiable basis for diagnostic applications, as shown in Fig. 1.

This review highlights recent advancements (2022–2025) in the design and application of PBA and PBE-based materials, organized around their responsiveness to glucose, ROS and

Hanna Mårtensson

Hanna Mårtensson graduated from Chalmers University of Technology in 2024 with a master's degree in biotechnology. She is currently conducting her PhD studies in the group of Associate Professor Alexandra Stubelius at Chalmers University of Technology. Her research focuses on improving polymeric nanomaterials for gene delivery.

Fan Jia

Fan Jia received her master's degree in biomedical engineering from Chalmers University of Technology in 2024. She completed her Master thesis in the group of Associate Professor Alexandra Stubelius and now continues her work as a project assistant within the same team. Her primary responsibilities include developing vessel-on a-chip models and image analysis.

Sia. We examine key mechanisms (Tables S1–S3), material architectures, and biomedical outcomes, and discuss how these boron-based chemistries can be applied in precision-guided therapeutic and theranostic platforms. Finally, we identify challenges and future directions to optimize their clinical relevance and utility in personalized medicine.

2. Glucose-responsive systems: towards adjustable and precise diabetes therapeutics

Diabetes, a global health crisis, currently affects an estimated 589 million people globally, with projections estimating more than 850 million cases by 2050. The disease is characterized by chronic dysregulation of blood glucose levels, which—if poorly managed—can lead to serious complications including cardiovascular disease, neuropathy, kidney failure, and vision loss. Despite the availability of insulin therapies, standard dosing regimens often fail to account for individual variability, resulting in suboptimal glycemic control and increased risk of hypoglycemia or hyperglycemia.[17] Glucose fluctuations vary widely among individuals and across disease states, influenced by time of day, disease type (Type 1 or Type 2), comorbidities, and lifestyle factors. This variability shows the need for personalized therapeutic platforms that can adapt to each patient's unique glucose profile in real time.

PBA-modified systems offer a promising solution. Through reversible covalent bonds with *cis*-diols, including glucose, materials respond proportionally to dynamic changes in glucose concentration. In aqueous environments, PBA exists in equilibrium between a neutral trigonal planar form and an anionic tetrahedral species, the latter of which readily forms ester bonds with glucose.[18] This dynamic binding behavior allows for biomarker-driven drug release, forming the basis of closed-loop, delivery systems that adjust dosing in response to real-time glucose levels. In healthy individuals, insulin is secreted by pancreatic β-cells to promote glucose uptake, storage and utilization.[19] In contrast, glucagon, secreted by α-cells, act as a counter-regulatory hormone that raises blood glucose levels during hypoglycemia by stimulating hepatic glucose production. In diabetes, both insulin and glucagon regulation are impaired, necessitating external administration. While insulin therapy has long been the cornerstone of diabetes management, glucagon delivery is increasingly recognized as essential for preventing and treating hypoglycemia, especially in closed-loop systems. Traditional approaches, such as subcutaneous injection, have been standard for over a century but often result in rigid dosing, poor patient adherence, and limited responsiveness to fluctuating glucose levels.[20] From a patient perspective, maintaining glucose balance is imperative, but so is ease of administration, minimizing complications, and improving quality of life. This section highlights how PBA/PBE-based materials are engineered to meet these clinical needs. By focusing on strategies for closed-loop insulin and glucagon regulation, hypoglycemia prevention, non-invasive administration, and treatment of diabetic comorbidities, we exemplify how PBA systems can support personalized diabetes care.

2.1. Strategies for closed-loop glucose management: mimicking pancreatic function

To simulate the feedback-driven insulin release of pancreatic β-cells, glucose-responsive materials must combine selective glucose recognition, controlled swelling or disassembly, and reliable payload retention.

Chen *et al.* (2022) developed a patient-friendly, closed-loop insulin delivery system using microneedles (MNs) composed of a PBA-functionalized porous hydrogel reservoir embedded in a polyvinyl alcohol (PVA)-coated tip **1** (Fig. 2a and Table S1.1).[21] This dual layered design enabled glucose-triggered insulin release while maintaining high mechanical strength and skin penetration efficiency. The porous hydrogel enhanced both drug loading capacity and interstitial fluid exchange (Fig. 2b–e), supporting dynamic responsiveness to glucose levels. Mechanistically, the porous gel base distributed

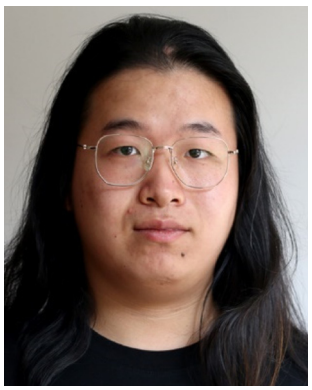

Yifan Gu

Yifan Gu is currently a biotechnology-master student at Chalmers University of Technology. He is conducting his master thesis in the group of Associate Professor Alexandra Stubelius at Chalmers University of Technology. His research focuses on synthesis and functionalization of hybrid nanoparticles applicable for target specific gene delivery.

Hamza Yakubu

Hamza Yakubu obtained a European Joint Master's degree in Bio and Pharmaceutical Material Sciences in 2023. He then joined Italian Institute of Technology Genova, Italy as a Research fellow in 2024. Currently, he is a PhD student in the group of Associate Professor Alexandra Stubelius at Chalmers university of technology. His research focuses on the development of hybrid nanomaterials for dual-modal imaging and drug targeting.

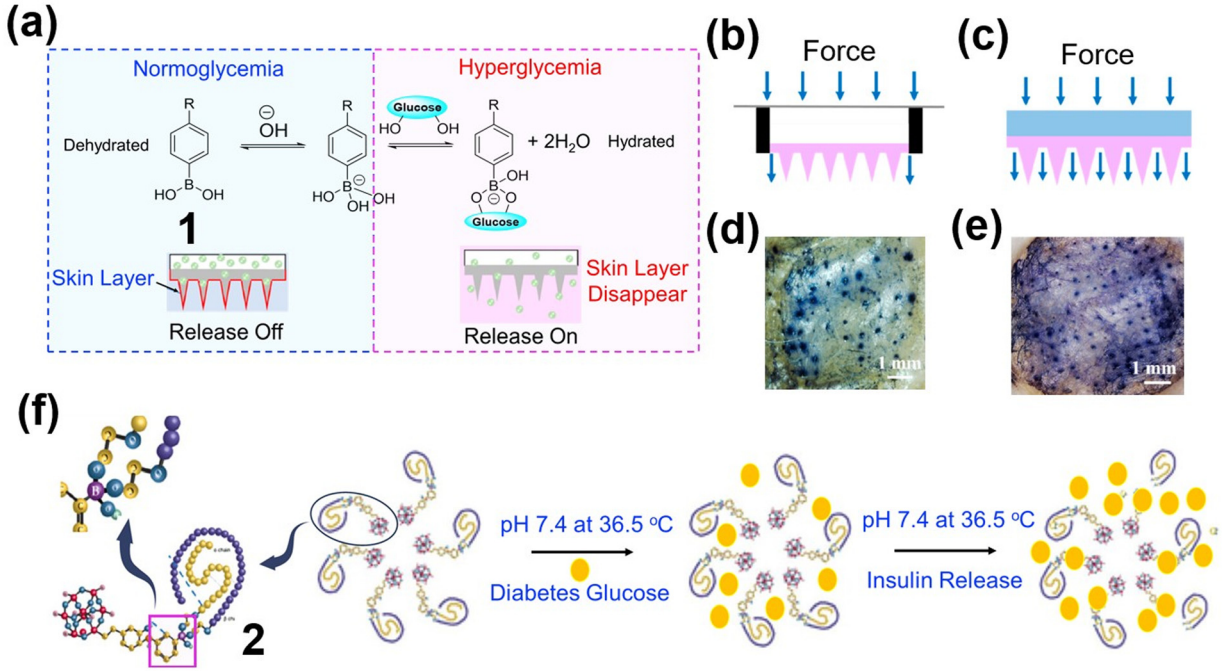

Fig. 2 Therapeutic strategies utilizing glucose binding mechanism of PBA. (a) Schematic representation of chemical constituents in **1**. (b) & (c) Illustration of mechanical strength of **1**. (d) & (e) Mice model experiments depicting the transdermal efficacy of 1 for delivering insulin. Reproduced from ref. 21 with permission from MDPI, copyright 1996–2025. (f) Constitution of **2** and its mechanism for insulin release. Reproduced from ref. 22 with permission from Springer Nature, copyright 2025.

insertion forces evenly, reinforcing the microneedles, while the crystallized PVA coating further increased tip strength to well above the level needed for transdermal delivery. Insulin was efficiently loaded into the reservoir *via* capillary action and transported to the needle tips for release. Glucose sensitivity was achieved through PBA moieties in the hydrogel tips, which reversibly bound glucose. Elevated glucose concentrations disrupted internal crosslinks, loosening the gel matrix and accelerated insulin diffusion. Conversely, lower glucose levels restored the network structure and slowed release. Additionally, a "skin-layer" effect within the gel helped regulate diffusion, ensuring controlled delivery under physiological conditions.

Kim *et al.* (2022) created nano-micelles using polyhedral oligosilsesquioxane (POSS) as a hydrophobic core and 3-aminophenylboronic acid (APBA)-linked insulin-PEG diols for shell formation **2** (Fig. 2f and Table S1.1).[22] Upon glucose exposure, PEG–diol–PBA interactions were disrupted *via* the reversible

Gizem Erensoy

Gizem Erensoy earned her PhD degree (Pharmaceutical Chemistry) from Marmara University, Istanbul in 2020. Afterwards, she joined Chalmers University of Technology as a postdoctoral researcher in Associate Professor Alexandra Stubelius's research group where she worked on the development of biomaterials for treating inflammation-related conditions. Currently she is working as research engineer at Chalmers University of Technology.

Alexandra Stubelius

Alexandra Stubelius is an Associate Professor at the Area of Advance Nano and at the Life Sciences Department, Chalmers University of Technology. She holds a Ph.D. in Medicine from the Department of Rheumatology and Inflammation Research and an M.Sc. Pharmacy from the Sahlgrenska Academy, University of Gothenburg. Following a postdoctoral fellowship at UC San Diego's Center of Excellence in Nanomedicine in the U.S., she established her research group, which focuses on deciphering immunological signaling to develop diagnostic tools, therapeutic materials, and disease models for inflammatory conditions.

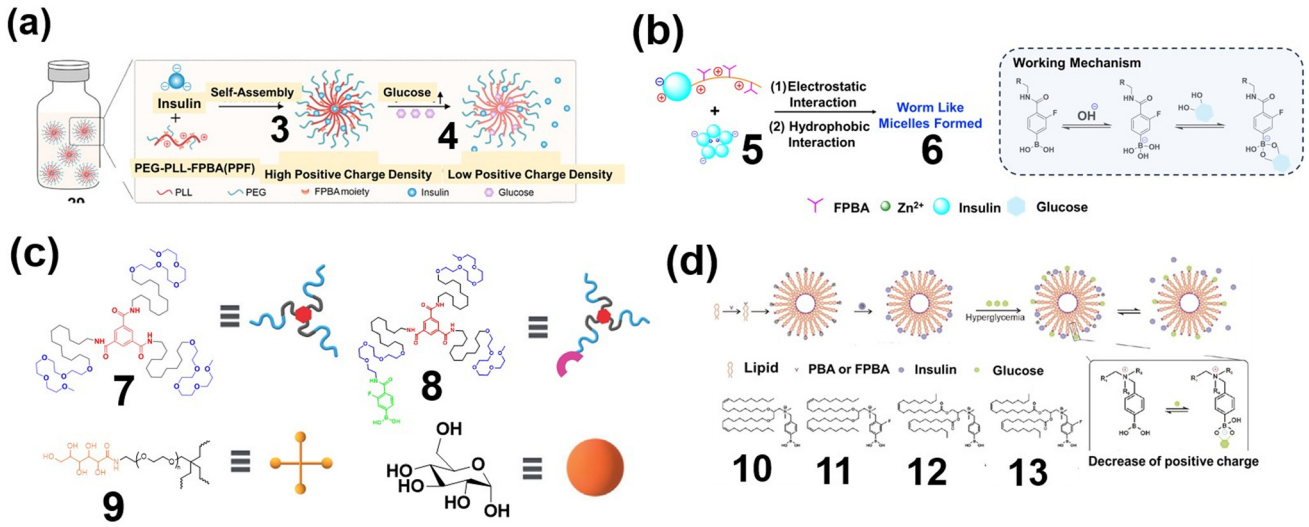

Fig. 3 Micellar nanoparticles capable of binding with PBA, thereby improving therapeutic efficacy in diabetes patients. (a) Schematic illustration of preparation and working mechanism of **3**. Reproduced from ref. 23 with permission of Elsevier. (b) Illustration of the worm like structure formed by of **6** by the constituents in **5**. (c) Schematic illustration providing the constituents **7–9**. Reproduced from ref. 25 with permission of Wiley. (d) Preparation of PBA derived nanomaterials **10–13**. Reproduced from ref. 26 with permission from Wiley, copyright © 1999–2025.

bonding between insulin-linked PEG diols and displacement by free glucose, triggering insulin release. This structural modularity allowed precise control over micelle formation and disassembly. Wang *et al.* (2023) developed 4-carboxy-3-fluorophenylboronic acid (FPBA)-modified polylysine micelles that together with PEG formed nano-sized insulin complexes (NIC) **3** (Fig. 3a). The construct achieved rapid reduction in hyperglycemia (within 30 minutes), which was maintained for 20 hours.[23] A follow-up construct by the same group (Ji *et al.* 2024) featuring FPBA and polycarboxybetaine encapsulated insulin and formed worm-shaped micelles **5** (Fig. 3b and Table S1.1) and established a liver insulin reservoir mimicking endogenous gradients, effective for up to 24 hours in a pig model.[24] The amphiphilic block design enabled localization and delayed release, with the FBA units acting as both glucose sensors and reversible cross linkers. VandenBerg *et al.* (2024) developed a hydrogel by crosslinking benzenetricarboxamide (BTA) to PBA to form a multiarm-crosslinker **7** (Fig. 3c), which not only enhanced the mechanical strength of the supramolecular hydrogel, but also facilitated a unique response to glucose. Glucose binding altered hydrogen bonding and charge distribution within the gel, leading to mechanical softening and controlled insulin diffusion.[25]

Wang *et al.* (2023) also introduced PBA-linked quaternary amine-type cationic lipids **10–13** (Fig. 3d and Table S1.1), which self-assembled in aqueous environments with insulin to form heterostructured nanoparticles. Under hyperglycemic conditions, these particles gradually reduced surface charge, weakening insulin–lipid interactions and enabling controlled release. This electrostatically modulated release profile proved effective in type 1 diabetic mouse models, offering another route to closed-loop delivery.[26] These constructs harness glucose-responsive boronate ester chemistry and reversible network disassembly to achieve physiologically aligned insulin release.

2.2. Minimizing hypoglycemia risk: glucose-triggered glucagon delivery

Both pre-clinical and clinical research have recently led to the development of glucagon-based therapeutic platforms aimed at preventing and treating hypoglycemia.[27] Unlike insulin delivery systems, which respond to elevated glucose levels, inverse glucose responsive systems are designed to remain inactive under normoglycemic conditions and activate only during hypoglycemic stress. PBA-functionalized hydrogels and micelles have been designed to leverage the reversible binding properties of PBA with glucose. When glucose levels drop, the weakened PBA–glucose interactions trigger material disassembly or gelation, leading to controlled glucagon release.

Yu *et al.* (2024) developed self-assembling nano-coils modified with PBA, **14** (Fig. 4a and Table S1.2).[28] These formed entangled β-sheets networks under normoglycemia, which disassembled upon glucose depletion. Mechanistically, the interactions between the PBA motifs and glucose stabilized and elongated the structure and induced gelation at physiological pH, which provided an inverse switch for glucagon release. Vinciguerra *et al.* (2024) designed PBA-containing micelles with covalently tethered glucagon **15** (Fig. 4b).[29] Under low glucose, reduced diol competition caused micelle destabilization, releasing active hormone with minimal cytotoxicity. Chen *et al.* (2025) further developed a supramolecular amphiphile peptide modified with a glucose-responsive PBA unit to achieve targeted glucagon delivery. The reversible binding between PBA and glucose controlled the electrostatic interactions and network cohesion of **17**, resulting in fine-tuned glucagon dosing in response to glycemic levels (Fig. 4c and

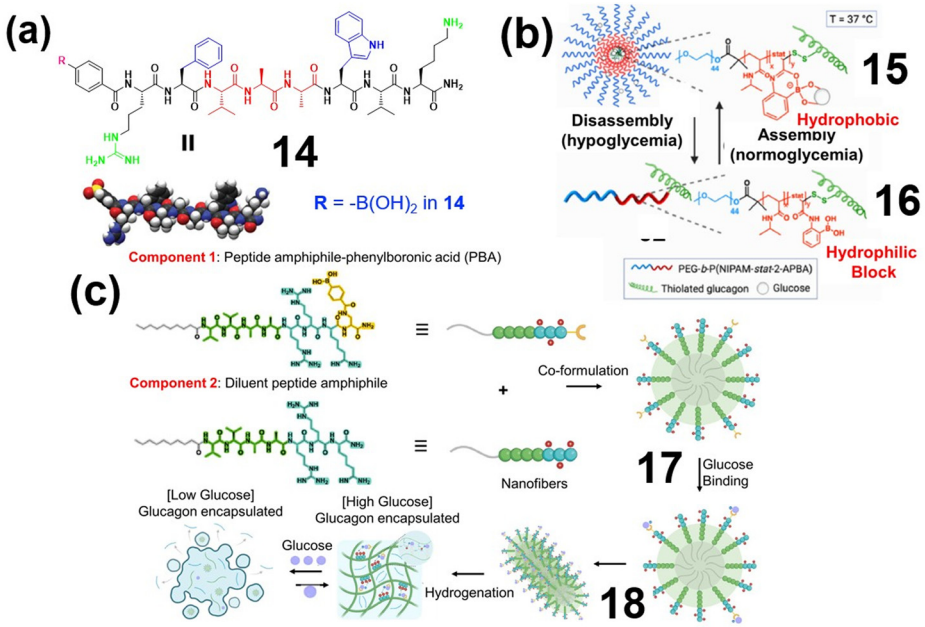

Fig. 4 Nanomaterials capable of glucose triggered therapeutic delivery of glucagon. (a) Chemical structure of **14**. Reproduced from ref. 28 with permission from Wiley. (b) Chemical structure and constituents present in **15**. Reproduced from ref. 29 with permission from ACS. (c) Preparation of nanoparticles **17** and **18** their glucose binding mechanism. Reproduced from ref. 30 with permission of Wiley, copyright © 1999–2025.

Table S1.2).[30] These systems used structural reversibility *via* hydrogen bonding, charge changes, or PBA–diol equilibrium shifts to achieve smart rescue therapy.

2.3. Improving patient adherence: non-invasive and long-acting systems

Non-injectable or injectable yet long-acting glucose-responsive formulations often improve patient adherence, particularly in chronic management. This can be achieved by reducing the invasiveness of the delivery route or developing extended-release strategies.

Shen *et al.* (2022) used fragment-based drug discovery to design fatty acid-modified polymeric nanocarriers with PBA motifs **20** (Fig. 5a and Table S1.3).[31] These systems provided circadian-aligned nocturnal insulin release in diabetic rats, lowering hypoglycemia risk and improving overnight glucose control. Saha *et al.* (2024) introduced multipolymer hydrogels (MPHGs) formed through *in situ* mixing of FPBA, polyethyleneimine, and PVA **21** (Fig. 5b).[32] By varying FPBA isomers (2FPBA, 3FPBA, 4FPBA), they tuned crosslinking density and mechanical strength. During the gelation process, molecular cargos were encapsulated within these hydrogels. These injectable, self-healing hydrogels showed glucose responsiveness and potential for customized depot formulation.

Yang *et al.* (2024) advanced dual-responsive hydrogel systems with glucose and pH sensitivity, enabling adjustable pore size and insulin release rates tailored to biomarker conditions. By conjugating APBA onto the skeleton of poly-L-lysine isophthalamide (PLP), they created PLP–PBA polymers (**23**) (Fig. 5c and Table S1.3).[33] The polymers were cross-linked with L-lysine methyl ester (LME), resulting in a hydrogel with tunable swelling properties depending on PBA grafting degree, and addresses the challenge of high pK_a associated with PBA. The dynamic network expanded pore size with elevated glucose, promoting controlled insulin release tailored to ambient metabolic states. These injectable hydrogels showed self-healing and pH/glucose co-responsiveness, preserving insulin bioactivity during administration and tissue integration.

For oral delivery, Ying *et al.* (2024) synthesized a hydrogel by modifying carboxymethyl agarose with 3-APBA and L-valine (referred to as CPL).[34] The hydrogel system **24** (Fig. 5d and Table S1.3) could overcome intestinal absorption barriers while enabling glucose-responsive insulin release and β-cell regeneration *in vivo*. Li *et al.* (2024) developed a multi-responsive oral insulin delivery system by conjugating PBA with poly (2-hydroxyethyl methacrylate) and poly(carboxybetaine) (PCB) **25** (Fig. 5e).[35] The formulated nanoparticles were loaded with glucose oxidase (GOx) and insulin. These particles degraded under low pH and high H_2O_2, releasing insulin in oxidative environments such as the gut mucosa. PCB's zwitterionic character facilitated epithelial penetration. When **25** was administered orally as capsules **25**, the bioavailability reached 20.24%, resulting in a hypoglycemic effect that lasted longer compared to intravenously injected insulin.

Another orally developed system was presented by Chen *et al.* (2025), who synthesized carboxymethyl chitosan (CMC) grafted with 3-APBA, forming a core–shell structure functionalized with citrus pectin spheres **26** (Fig. 6 and Table S1.4).[36] These CMC–APBA core–shell nanoparticles encapsulated arte-

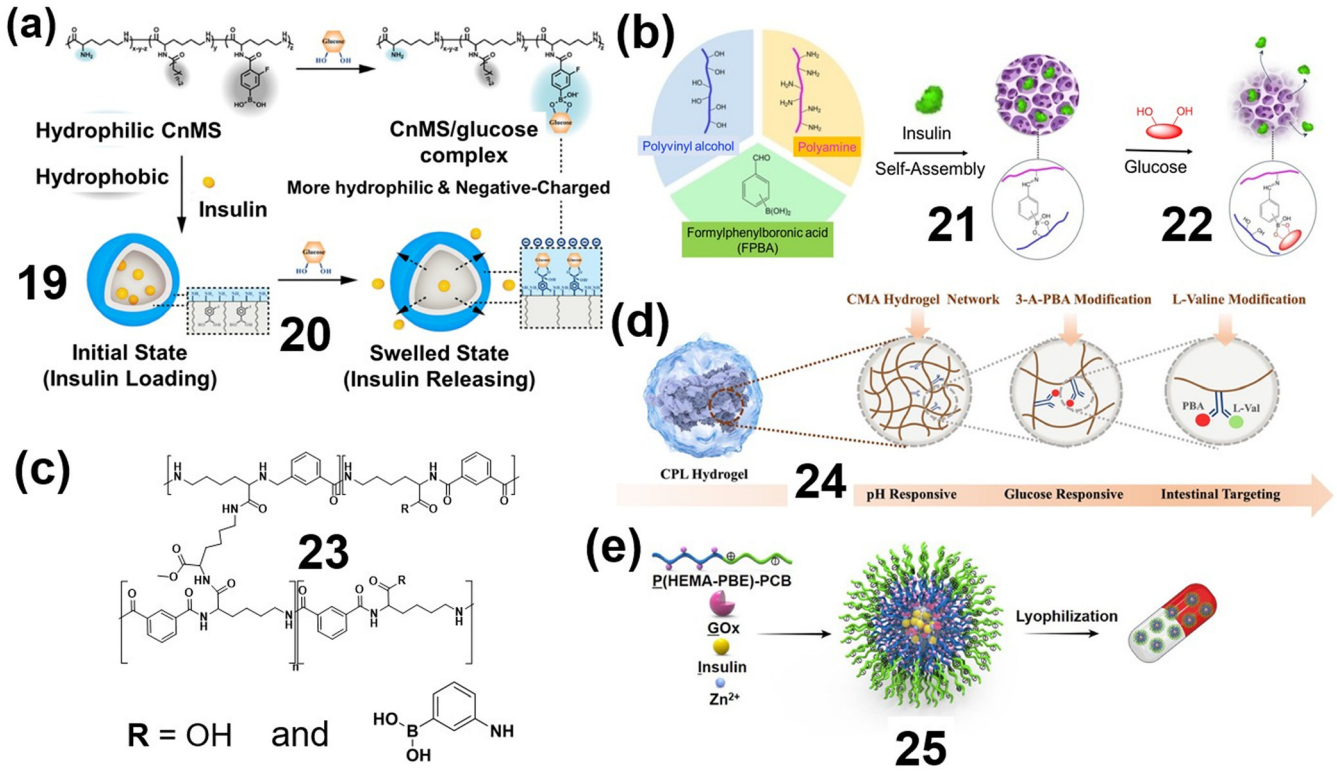

Fig. 5 Glucose-responsive insulin delivery systems for enhancing patient adherence in diabetes management. (a) Chemical structure and modifications of nanoparticles with insulin **19** and insulin release mechanism **20**. Reproduced from ref. 31 with permission from Elsevier. (b) Structure and working mechanism of hydrogel **21**. Reproduced from ref. 32 with permission from Wiley. (c) Chemical structure of polymer **23**. Reproduced from ref. 33 with permission from RSC. (d) Internal structure of hydrogel nanoparticles **24**. Reproduced from ref. 34 with permission from ACS. (e) Self-assembly based nanoparticles **25** and capsule formation. Reproduced from ref. 35 with permission from Theranostics, copyright © 2025 open access.

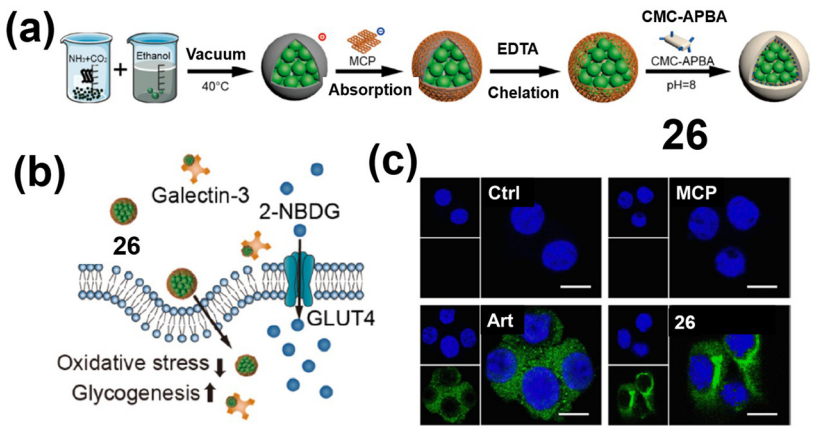

Fig. 6 Orally delivered artemisinin using chitosan grafted PBA materials. (a) Synthesis of **26**. (b) Mechanism of insulin resistance in HepG2 cells treated with **26**. (c) Insulin immunofluorescence of pancreatic α-cells treated with MCP, Art and **26** for 72 h. Reproduced from ref. 36 with permission from Elsevier, copyright © 2025.

misinin (Art), a drug that promotes β-cell regeneration and mitigates insulin resistance.[37] The borate ester linkage enabled glucose-triggered Art release, targeting inflammation and oxidative stress by downregulating the proinflammatory pathway NF-κB, amongst other. *In vivo* experiments revealed that treatment with **26** resulted in reduced blood glucose levels, decreased inflammation, lower oxidative stress, and reversed insulin resistance in rat models (Fig. 6b and c). Additionally, signs of pancreatic β-cell regeneration were observed.

2.4. Targeted management of diabetic complications

Diabetes is a systemic disease with widespread metabolic and inflammatory consequences. Next-generation PBA/PBE materials are being developed not only for glycemic control but also to address secondary complications such as chronic inflammation and nephropathy. Among these, diabetic wound care has emerged as a particularly active and promising area of research, where glucose-responsive biomaterials offer site-specific, dynamic therapeutic delivery tailored to the wound microenvironment.

Chronic, non-healing wounds such as diabetic foot ulcers pose a major clinical challenge, exacerbated by local hyperglycemia, oxidative stress, microbial infection, and persistent inflammation. Several studies have demonstrated the potential of flavonoid- and polyphenol-loaded hydrogels for responsive antioxidant delivery. Collectively, they leverage PBA-based glucose sensing for precision delivery of anti-inflammatory, antioxidant, antimicrobial, or angiogenic agents where and when they are most needed. Xu *et al.* (2022) designed PBA-modified hyaluronic acid hydrogels loaded with myricetin **27** (Fig. 7a and Table S1.4) or catechin **29** (Fig. 7c).[38,39] These hydrogels released antioxidants in response to glucose and ROS, promoting wound healing by reducing oxidative damage. Liang *et al.* (2022) developed a pH/glucose dual-responsive hydrogel for metformin delivery, enhancing anti-inflammatory effects in inflamed diabetic wounds **30** (Fig. 7d and Table S1.4).[40] Liu *et al.* (2023) further advanced the field with a multifunctional hydrogel incorporating fulvic acid and EN106 to modulate redox signaling *via* the FEM1b–FNIP1 pathway **31** (Fig. 7e).[41]

Further targeting complications associated with mismanaged diabetes, several strategies target infection, angiogenesis, and renal dysfunction. Chen *et al.* (2023) introduced a supramolecular hydrogel with guanosine-hemin peroxidase activity **32** (Fig. 8a), converting glucose into H_2O_2 for bacterial sterilization.[42] Zhang *et al.* (2024) embedded MMP-9-sensitive

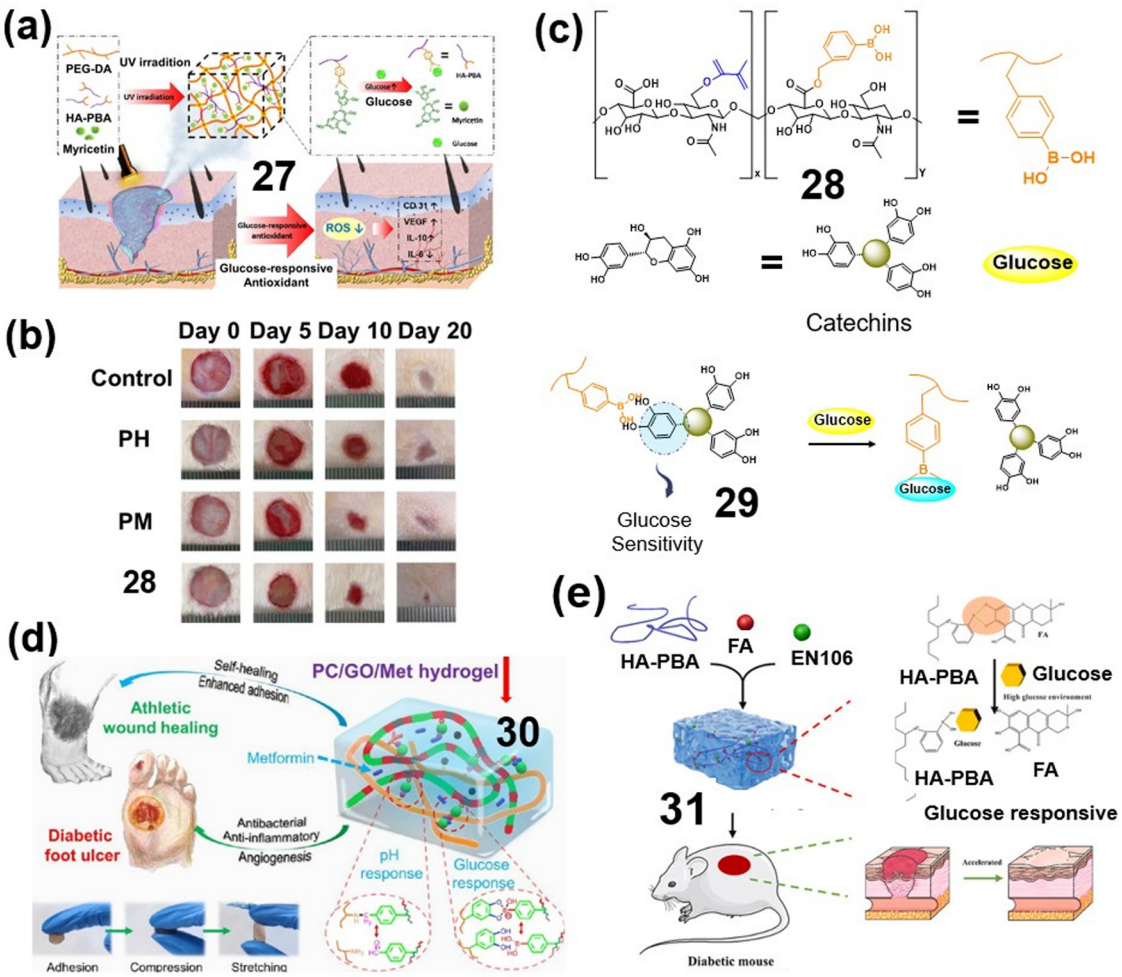

Fig. 7 Evaluation of glucose triggered diabetic wound healing systems in mice models. (a) Diagram Illustrating the mechanism of **27** hydrogel platform for diabetic wound healing. (b) Representative images of wound healing in mice models. Reproduced from ref. 38 with permission of Elsevier. (c) Schematic diagram showing the glucose-responsive antioxidant hydrogel platform **28–29** for diabetic wound healing. Reproduced from ref. 39 with permission of ACS. (d) Structure and glucose responsive mechanism of material **30**. Reproduced from ref. 40 with permission of ACS. (e) Synthetic approach for formation of **31** and application. Reproduced from ref. 41 with permission from Elsevier, copyright © 2025.

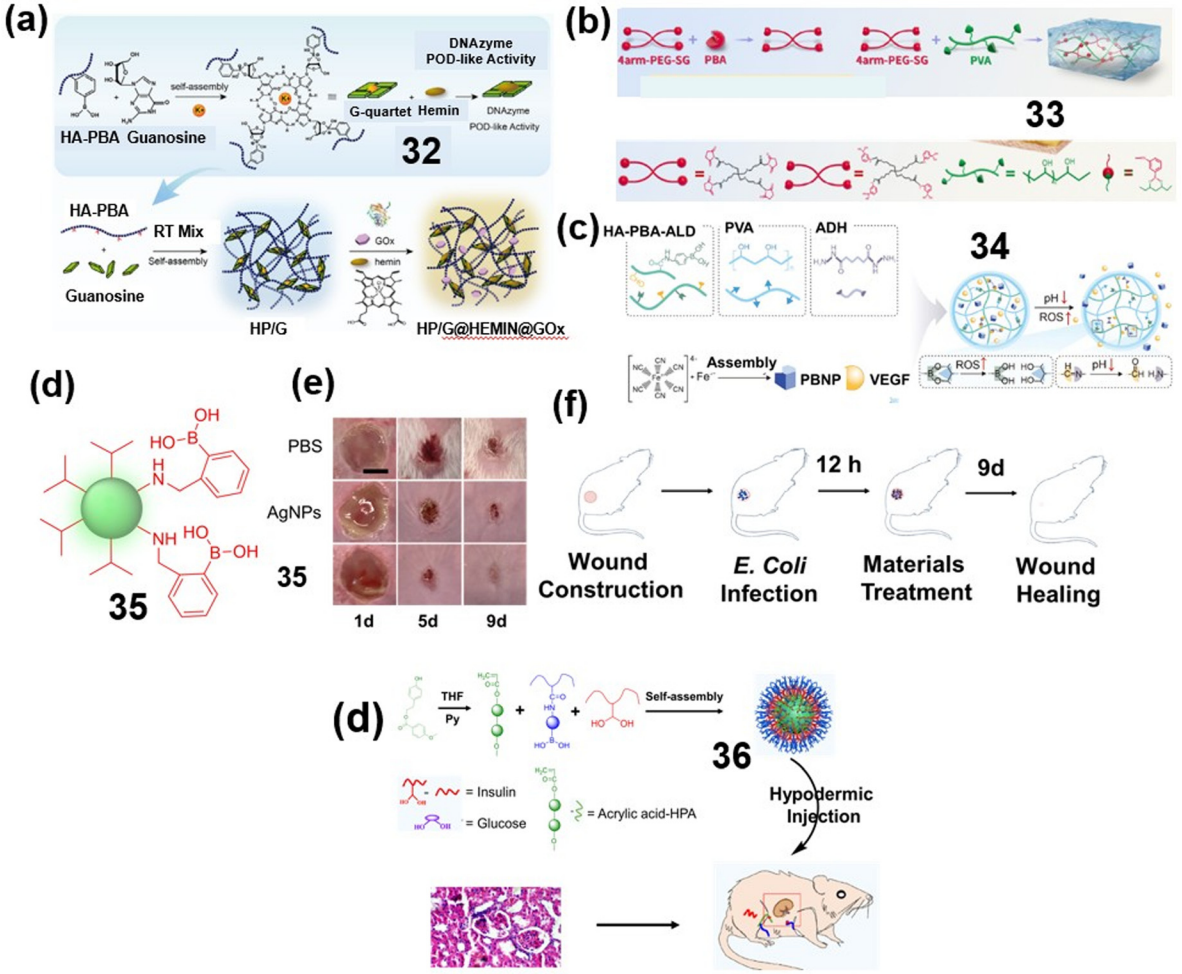

Fig. 8 PBA functionalized hydrogels for diabetic complications. (a). Diagram showing different constituents in **32**. Reproduced from ref. 42 with permission from Elsevier. (b) Synthetic scheme and components in **33**. Reproduced from ref. 43 with permission from Elsevier. (c) Different constituents involved in the development of **34**. Reproduced from ref. 44 with permission from Wiley. (d) Structure of **35**. (e) Representative images of *E. coli*-infected wounds with different treatments at defined time points. (f) The scheme of the *E. coli*-infected wound model and subsequent treatments. Reproduced from ref. 45 with permission from RSC. (g) Synthesis of drug delivery agent **36**, reproduced from ref. 46 with permission from Elsevier copyright © 2025.

microcapsules **33** (Fig. 8b) to guide the release of L-carnitine and diclofenac based on inflammatory signals.[43] Wang *et al.* (2024) co-delivered VEGF and Prussian blue nanoparticles, enabling targeted angiogenesis through a multi-trigger (pH/ROS/glucose) design **34** (Fig. 8c).[44] You *et al.* (2022) combined silver nanoparticles with PBA moieties **35** (Fig. 8d and Table S1.4), to selectively bind bacterial glycans, improving both wound sterilization and resolution.[45] For targeting renal dysfunction, Ma *et al.* (2022) created 3-(acrylamido)phenylboronic acid (AAPBA) block copolymers with the plant-extract *p*-hydroxyphenylethyl anisate (HPA) to form nanoparticles **36** with excellent glucose sensitivity and renal targeting (Fig. 7f).[46] The degradation released HPA for anti-inflammatory effects that restored filtration capacity in diabetic nephropathy models.

Each system leverages PBA conjugation, responsive network formation, or tissue-preferential targeting to manage secondary pathologies and enhance therapeutic effects.

2.5. Summary: PBA and PBE as glucose responsive materials in personalized medicine

PBA and PBE-based materials offer a dynamic and adaptable chemical platform for personalized diabetes management. As demonstrated across various studies, these chemistries have been successfully integrated into diverse architectures, including micelles, hydrogels, peptides, and nanoparticles, allowing for personalized, glucose-responsive drug delivery. The platforms are engineered around several key mechanistic principles, including dynamic covalent bonding with glucose *via* boronate ester formation, reversible network swelling or disassembly upon glucose binding, multi-responsive behavior when integrating secondary triggers like pH, redox state, or enzymatic activity, and tissue-targeting capabilities enabled by ligand-functionalized or organ-selective carriers.

Effective glucose recognition under physiological conditions requires boronic acid in its anionic form. Lowering the pK_a below ~7.5 ensures more efficient interaction with glucose *in vivo*. To achieve this, 3-aminophenylboronic acid (APBA) and 4-carboxy-3-fluorophenylboronic acid (FPBA) are commonly used. APBA offers water solubility and chemical stability, where the amine group allows for ease of conjugation. Similarly, FPBA with the fluorine group lowers the pK_a of boronic acid, enhancing its glucose responsiveness at physiological pH (~7.4). These glucose-responsive systems have evolved into finely tuned platforms capable of feedback-controlled drug release, adjusting insulin or glucagon delivery in real time based on fluctuating glucose levels. This enables closed-loop glucose management that mimics pancreatic function, reduces the risk of hypoglycemia through inverse-responsive glucagon release, and improves patient adherence *via* non-invasive and long-acting formats such as microneedles and oral hydrogels. Together, these strategies exemplify how biomarker-sensitive materials can enable intelligent, individualized interventions aligned with the principles of precision medicine.

3. ROS-responsive PBA and PBE materials: targeting oxidative stress in personalized therapies

Oxidative stress is a hallmark of diverse pathologies and varies by tissue type, disease stage, and individual patient conditions.[47,48] PBE-based materials respond to pathological ROS levels, making them suitable for personalized targeting of inflamed or cancerous tissues. There are three primary sites of endogenous ROS generation in the body: NADPH oxidase (NOX) on the surface of innate immune cells, mitochondria, and endoplasmic reticulum, all of which produce O_2^-. Additionally, transition metals and superoxide dismutases (SOD) contribute to the production of $^{\bullet}OH$ and H_2O_2 by reacting with H_2O_2 and O_2^-, respectively. Generally, excessive ROS levels can cause non-specific damage to lipids, proteins, and DNA, as well kill pathogens and bacteria, while low levels of ROS stimulate cell signal pathways and promote cell proliferation.[49] ROS levels in tumor cells and activated immune cells can be elevated up to 100×10^{-6} M,[47] which is 2 to 3 times higher than normal cells. We have previously shown that PBE-based materials are capable of scavenging ROS when the material is degraded.[50] Recent systems exploit ROS-triggered degradation to release therapeutics selectively within diseased microenvironments. By incorporating additional pH or enzymatic responsiveness, these dual-stimuli platforms exhibit improved control over spatial and temporal drug delivery. The tunability of ROS sensitivity can be modulated through boronate substituents, sterics, and hydrophobicity, allowing selective response thresholds for different tissue conditions. Matching ROS sensitivity to patient-specific oxidative stress markers enables therapies that are activated only under pathological conditions while remaining inert in healthy tissues. In this section, we exemplify how PBA/PBE-based platforms are being used to harness ROS for patient-specific targeting and real-time feedback in drug delivery and diagnostics.

3.1. Adjustable activation and site-selective therapeutic delivery in oxidative microenvironments

Increased oxidative stress is common in tumors, but also in inflammatory diseases. Here, it is especially important with site-specific drug release and activation only at the sites where the drugs are needed. Each example illustrates a distinct strategy to achieve redox-triggered drug delivery or tissue modulation.

Yin *et al.* (2024) designed a H_2O_2-activated prodrug **37** (Fig. 9a and Table S2.1) that was constructed by linking the cytotoxic agent amonafide (AMF) to a H_2O_2-responsive PBE moiety, enabling selective drug release. Upon exposure to H_2O_2, the PBE group was oxidized to a phenol, cleaving the prodrug linkage and releasing fluorescent, bioactive AMF. *In vitro* studies demonstrated a positive correlation between intracellular H_2O_2 levels and anticancer efficacy, with the prodrug showing enhanced activity in MDA-MB-231 breast cancer cells.[51]

Zhao *et al.* (2022) developed an injectable chitosan-based hydrogel **39** incorporating boronate-protected diazeniumdiolate (CS-B-NO) to regulate the ROS/NO balance after myocardial ischemia/reperfusion (I/R) injury (Fig. 9b and Table S2.1). In ROS-rich post-infarct tissue, boronic acid groups were oxidized by H_2O_2, releasing nitric oxide (NO) in a site-specific manner. This restored antioxidant signaling and activated the Nrf2-Keap1 pathway while inhibiting NF-κB-mediated inflammation, resulting in reduced cardiac damage and improved ventricular remodeling in a mouse model of myocardial infarct (MI). Unlike static NO donors, hydrogel 39 offered adaptive NO release in response to local oxidative stress, supporting tissue repair and cardioprotection.[52]

Gao *et al.* (2022) constructed a biodegradable antioxidant hydrogel (**40**, Fig. 9c and Table S2.1) from a Schiff base reaction between oxidized dextran (Ox-Dex), adipic acid dihydrazide (ADH), and PBA-grafted hyaluronic acid (HA–ADH–PBA). This formulation provided ROS scavenging *via* boronate ester cleavage, protecting infarcted myocardium from oxidative damage in both short- and long-term studies. *In vivo*, hydrogel 40 reduced lipid peroxidation and inflammatory cell infiltration, promoted angiogenesis, and preserved cardiac contractility. Molecular analyses confirmed regulation of pro-inflammatory gene expression and improved cardiomyocyte viability over an 8-week period, demonstrating its therapeutic potential in post-MI recovery.[53]

Jia *et al.* (2023) introduced a ROS-activated supramolecular nanoassembly **41**, Fig. 9d, incorporating ethyl caffeate-stabilized PBE for the treatment of acute kidney injury (AKI). The nanoassemblies were functionalized with L-serine, enabling active targeting to damaged renal tissue *via* Kidney Injury Molecule-1 (Kim-1) binding. Upon exposure to pathological ROS levels, the PBE linkers degraded, releasing 4-hydroxybenzyl alcohol and ethyl caffeate, two potent antioxidants. These agents effectively suppressed oxidative damage and acute inflammation, preserving renal function.[54]

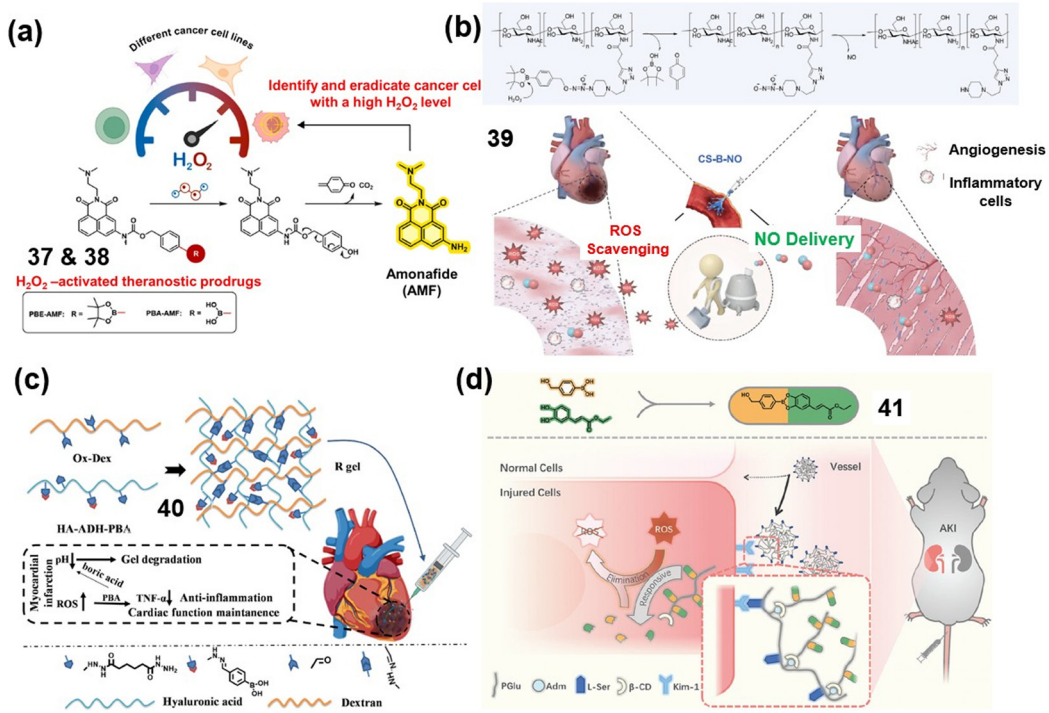

Fig. 9 PBA bound organic and nanomaterials for therapeutics in oxidative microenvironments. (a) Schematic illustration of mechanism of ROS responsive drug delivery system **37** for cancer therapeutics. Reproduced from ref. 51 with the permission from Elsevier. (b) Combination and working strategy for development of **39**. Reproduced from ref. 52 with permission from Wiley. (c) Self-assembled hydrogel **40** its constituents and treatment of myocardial infarction. Reproduced from ref. 53 with permission from Elsevier. (d) Preparation of nano-assembly **41** and biomedical application of the developed materials. Reproduced from ref. 54 with permission from Wiley, copyright © 1999–2025.

3.2. Dual and multi-responsive systems for precision control

By integrating ROS sensitivity with additional triggers such as pH, or enzymatic activity these systems achieve precision control, enhancing both specificity and efficacy in complex biological settings. Zhao *et al.* (2024) constructed a dual pH- and ROS-responsive micellar nanoformulation **42** (Fig. 10a and Table S2.2) by conjugating PBA and folic acid (FA) to glycol chitosan (GC), followed by doxorubicin (DOX) loading. The micelles remained stable under physiological conditions but accelerated drug release in acidic and oxidative tumor microenvironments. FA facilitated receptor-mediated uptake in HepG2 cells, while PBA conferred sensitivity to ROS and pH. This triggered degradation strategy enabled precise intracellular release of DOX, significantly inhibiting cell migration and proliferation *in vitro*. The dual-responsiveness of 42 exemplifies targeted payload delivery through environmental cues, offering improved selectivity and reduced off-target toxicity.[55]

For inflammatory vascular conditions, Zhang *et al.* (2022) introduced multi-bioactive micelles **43** (Fig. 10b and Table S2.2) targeting abdominal aortic aneurysm (AAA). These micelles self-assembled from PBE, ROS-scavenging TEMPOL, and PEG amphiphiles. The micelles accumulated in neutrophils, macrophages, and vascular smooth muscle cells (VSMCs) within AAA tissue, where elevated ROS and inflammation triggered on-demand degradation. By concurrently delivering rapamycin and neutralizing ROS, 44 provided multi-targeted protection against inflammation, calcification, and apoptosis in VSMCs.[56]

Liu *et al.* (2022) created a dual pH/ROS-responsive injectable hydrogel **44** (Fig. 11a and Table S2.2) composed of a boronic ester and imine-crosslinked matrix containing SS31-modified micelles encapsulating cyclosporine A (CsA). In ischemia/reperfusion (I/R) cardiac injury, the acidic and oxidative conditions degraded the hydrogel matrix, releasing mitochondria-targeted micelles. The system facilitated hierarchical ROS scavenging: the PBE module eliminated cytosolic ROS, while SS31 neutralized mitochondrial oxidative stress. This spatiotemporally controlled release preserved mitochondrial integrity, reduced apoptosis, and improved cardiac function in rat I/R models—demonstrating dual-responsive precision in cardiac therapeutics.[57]

Guo *et al.* (2023) designed hydrogel **45** (Fig. 11b) integrating catechol adhesives and a dynamic PBE-based glucose/ROS-responsive matrix, loaded with photothermal antibacterial TP@AgNPs. The hydrogel exhibited self-healing, injectability, and firm tissue adhesion, enabling deep wound integration. Elevated glucose and ROS levels in diabetic wounds triggered hydrogel degradation and selective antimicrobial agent release, promoting M2 macrophage polarization and ROS scavenging. *In vivo*, **45** accelerated healing of infected wounds with minimal systemic toxicity.[58]

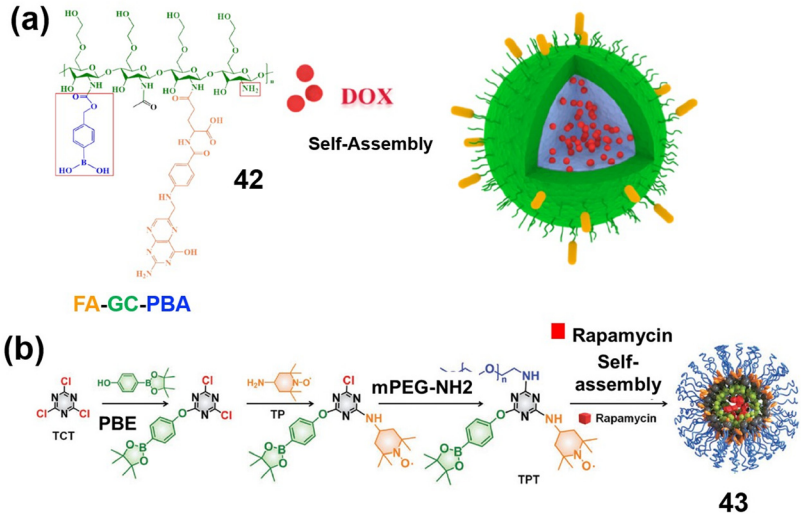

Fig. 10 Dual responsive self-assembled materials consisting of PBA and PBE groups for therapeutics in oxidative stress environments. (a). Schematic illustration of self-assembly of material **42** for delivering DOX. Reproduced from ref. 55 with permission from ACS. (b) Self-assembly strategy for construction of **43**. Reproduced from ref. 56 with permission from Wiley, copyright © 1999–2025.

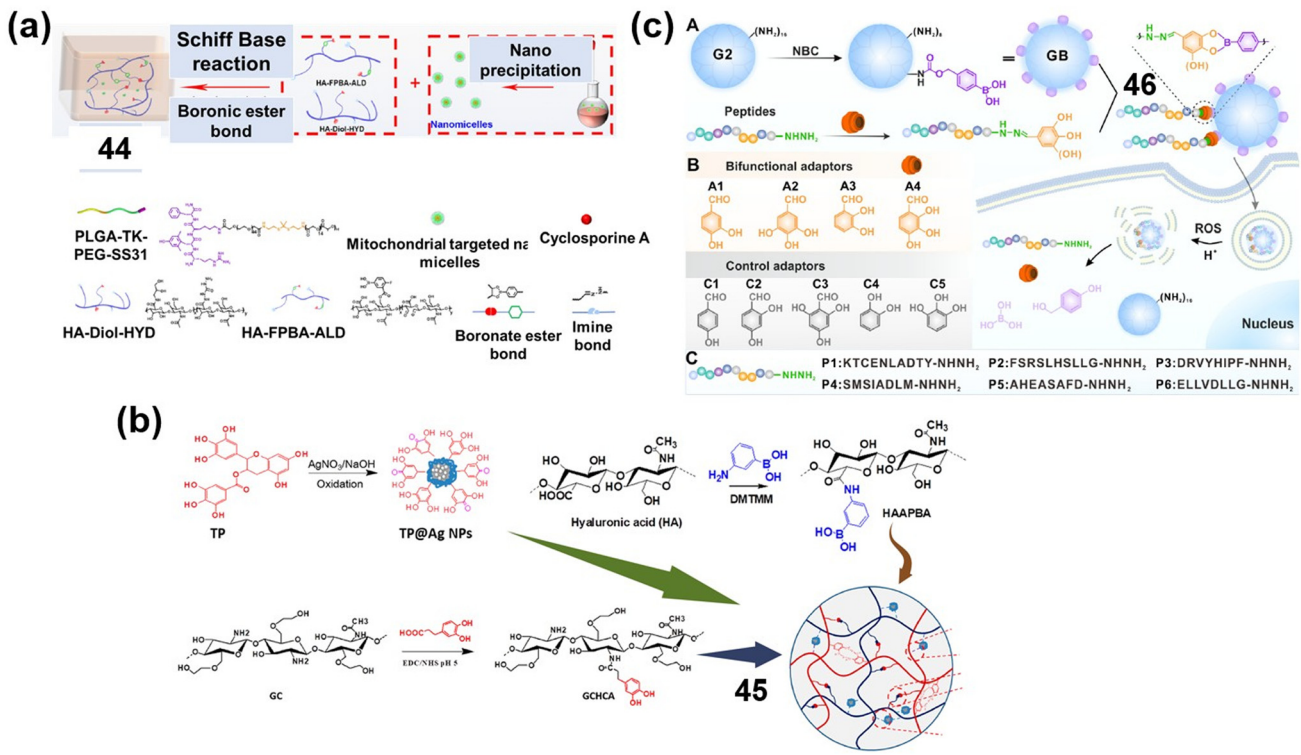

Fig. 11 PBA and PBE loaded dual responsive hydrogels for therapeutic application in oxidative stress microenvironments. (a) Preparation and structural composition of hydrogel **44**. Reproduced from ref. 57 with permission from Elsevier. (b) Different steps involved in the synthesis of **45**. Reproduced from ref. 58 with permission from ACS. (c) Structural composition and peptide delivering mechanism utilized by **46**. Reproduced from ref. 59 with permission from Elsevier, copyright © 2025.

Rong *et al.* (2023) developed bioconjugates **46** (Fig. 11c and Table S2.2) for peptide delivery by integrating catechol and aldehyde functionalities into a PBA-linked dendrimer scaffold. Peptides were conjugated *via* ROS-cleavable catechol-boronate and pH-labile hydrazone linkages. Upon exposure to intracellular ROS and acidic endolysosomal environments, the linkages disassembled, triggering selective peptide release into the cytosol. These bioconjugates efficiently delivered pro-apoptotic

peptides into osteosarcoma cells *in vitro* and *in vivo*, exhibiting targeted tumor growth inhibition while avoiding systemic peptide diffusion.[59]

3.3. On-demand degradation to minimize systemic toxicity

PBA and its analogs can leverage redox-triggered degradation for precise, localized treatment while minimizing off-target effects and systemic toxicity. To improve antigen-specific immune responses while avoiding systemic immune overstimulation, Wang *et al.* developed a ROS- and pH-responsive nanovaccine **47** (Fig. 12a and Table S2.3) composed of TRP2 tumor antigen peptides conjugated to a PBE-modified PEG-*b*-PAsp copolymer.[60] The nanostructure exhibited enhanced lymph node targeting and dendritic cell uptake due to its negative surface charge. Upon entry into ROS-rich antigen-presenting cells, the boronate esters were oxidized, releasing TRP2 and degradation byproducts in a controlled intracellular manner. This degradation allowed for spatiotemporally confined antigen release, thereby minimizing off-target immune activation. *In vivo*, this led to potent $CD8^+$ T cell responses, tumor growth suppression, and improved survival without the need for external adjuvants.

Zhao *et al.* (2025) formulated a dual-functional, ROS-sensitive hydrogel **48** (Fig. 12b and Table S2.3) from 8-aminoguanosine (8AG) and 1,4-phenylenediboronic acid (PDBA) for the treatment of inflammatory periodontal disease. The PDBA served as an antioxidant linker, while 8AG modulated macrophage signaling (MAPK and NF-κB) to reduce inflammation. The hydrogel degraded *in situ* under oxidative stress, releasing immunomodulatory agents in a localized, time-controlled fashion. In mouse models, it reduced M1 macrophage polarization and inhibited osteoclast activity, thereby minimizing alveolar bone loss, demonstrating local immunotherapy.[61]

To enhance chemotherapy–immunotherapy synergy while reducing systemic exposure, Liang *et al.* engineered a ROS-degradable hydrogel **49** (Fig. 12c and Table S2.3) to co-deliver gemcitabine and the STING agonist DMXAA directly to the tumor site. The hydrogel was constructed with ROS-labile crosslinkers that selectively degraded in the oxidative tumor microenvironment. This spatial control limited systemic dissemination of immunostimulatory agents, reducing inflammation outside the tumor. In a postsurgical pancreatic tumor model, hydrogel **49** promoted innate immune activation, T-cell infiltration, and long-term tumor suppression.[62]

To reduce systemic toxicity in psoriasis therapy, Zhu *et al.* created microneedle patches (**50**, Fig. 12d) integrating a PBA-modified hydrogel with methotrexate (MTX) and epigallocatechin gallate (EGCG). The system employed dual-release mechanisms: passive diffusion for MTX and ROS-triggered, boronate-cleavage-mediated release of EGCG. By confining EGCG delivery to inflamed, H_2O_2-rich psoriatic skin, the system prolonged antioxidant action locally while reducing systemic drug burden. *In vivo*, the microneedles improved disease outcomes with lower dosing and reduced off-target effects.[63]

To target osteoarthritis (OA) pathology while avoiding joint-wide immunosuppression, Jiang *et al.* developed a bifunctional, ROS-responsive hydrogel system (**51**, Fig. 12e and Table S2.3). The system encapsulated siMMP-13-loaded Fe_3O_4 nanoparticles within a PBA-crosslinked hyaluronic acid/PVA matrix. In response to elevated ROS in inflamed cartilage, the hydrogel

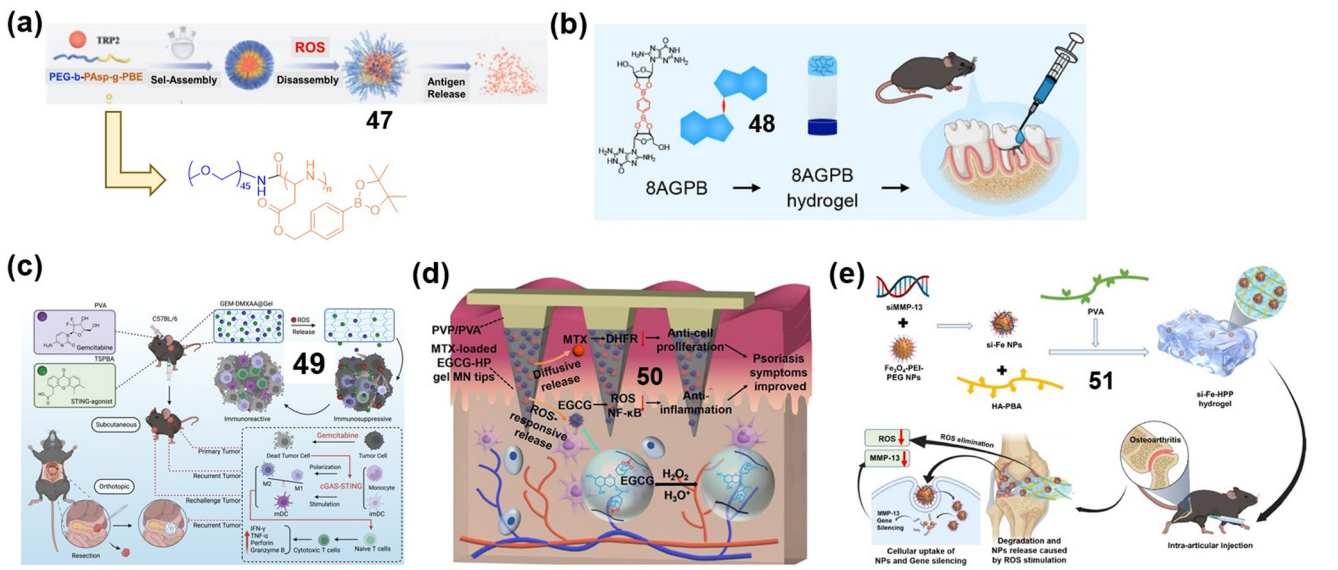

Fig. 12 Illustration of strategies used for decreasing toxicity of PBA and PBE loaded materials with therapeutic applicability. (a). Chemical combination of nano formulation **47**. Reproduced from ref. 60 with permission from Taylor and Francis. (b) Chemical structure and application of **48**. Reproduced from ref. 61 with the permission from Elsevier. (c) Schematic illustration of synthesis and bio-application of **49**. Reproduced from ref. 62 with permission from Wiley. (d) Preparation wound healing microneedle patches **50**. Reproduced from ref. 63 with permission from ACS. (e) Preparation of iRNA delivery hydrogel **51** and its application treating osteoarthritis. Reproduced from ref. 64 with the permission from BMC copyright © 2025.

matrix degraded, releasing RNAi agents locally to downregulate catabolic enzymes and reduce inflammation. Intra-articular administration showed minimal systemic spread, extended joint retention, and effective cartilage preservation.[64]

3.4. Protecting biological cargo using ROS-responsive PBA/PBE materials

Cytosolic delivery of native proteins, including enzymes, antibodies, and gene editors, has transformative implications for precision therapies yet remain limited by premature degradation and lack of stimuli-responsive control. PBA and PBE-based polymers address these challenges by forming dynamic, ROS-sensitive linkages that enable site-selective release in oxidative disease microenvironments such as tumors. The following examples illustrate how structural modularity—ranging from nitrogen–boronate coordination to dual-functional ligand grafting—enables programmable intracellular trafficking, controlled degradation, and effective protein therapeutic action.

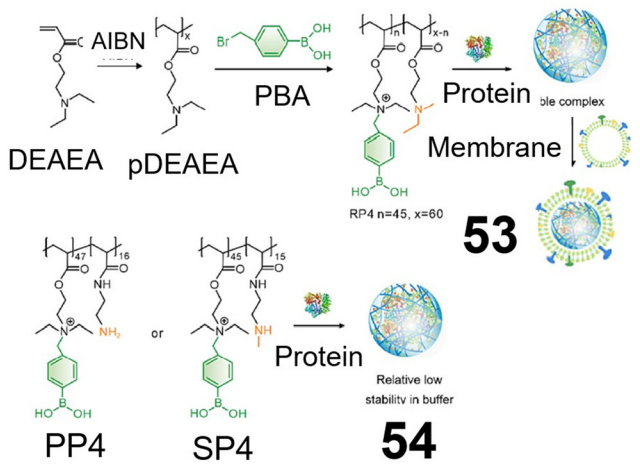

Fig. 13 ROS responsive PBA based self-assembled nanomaterials for safe delivery of biological cargo to disease affected regions. Synthesis of nano formulation **53** and **54**. Reproduced from ref. 66 with permission from Elsevier, copyright © 2025.

To safely deliver intracellular protein therapeutics, Yin *et al.* formulated EPP–protein nanocapsules (NCs, **52** and Table S2.4) by grafting PEI, EGCG, and 2-APBA onto therapeutic proteins. The capsules remained stable in circulation due to reversible boronate ester and imine bonds, which underwent cleavage inside ROS- and acid-rich endo–lysosomes, enabling cytosolic protein release only at the target site. This modular design supported precise delivery of enzymes, antibodies, and CRISPR-Cas9 RNPs, surpassing commercial transfection reagents. *In vivo*, subcutaneously injected EPP–saporin NCs localized drug action to tumors while sparing normal tissues.[65]

Cheng *et al.* (2023) developed ROS-sensitive polymers rich in boron units *via* radical polymerization and post-modification strategies. The resulting polymers (**53**, **54**, Fig. 13 and Table S2.4) formed stable complexes with cargo proteins through boronate-mediated coordination and electrostatic interactions. Notably, polymer **55** demonstrated enhanced cytosolic release of saporin in tumor models due to its optimized amine-to-boron ratio and ROS-induced polymer disassembly, allowing for intracellular delivery while maintaining protein activity.[66]

Yin *et al.* (2023) introduced a dual-responsive cytosolic protein delivery platform based on nucleoside-conjugated PBA chemistry. To mimic the structural and electrostatic features of nucleic acids, they synthesized adenylated pro-proteins (A-proteins) with highly negative surface charges. These were electrostatically and complementarily paired with thymidine-modified PEI, forming stable nanocomplexes **55** (Fig. 14a and Table S2.4) *via* PBA-based ester linkages.[67] The resulting complexes exhibited strong resistance to physiological salts and

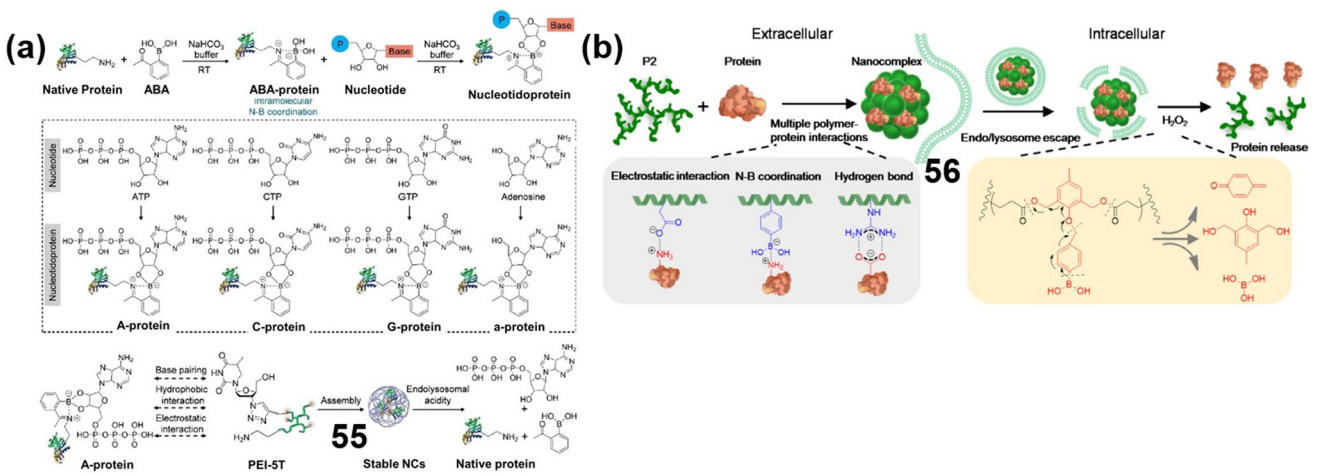

Fig. 14 Biocompatible self-assembled nanomaterials integrating biologically relevant molecules with PBA components for the safe delivery of therapeutic cargo. (a) Process for the preparation of A-protein based NCs **55**. Reproduced from ref. 67 with permission from Wiley. (b) Chemical components and working mechanism of **56**. Reproduced from ref. 68 with permission from Elsevier, copyright © 2025.

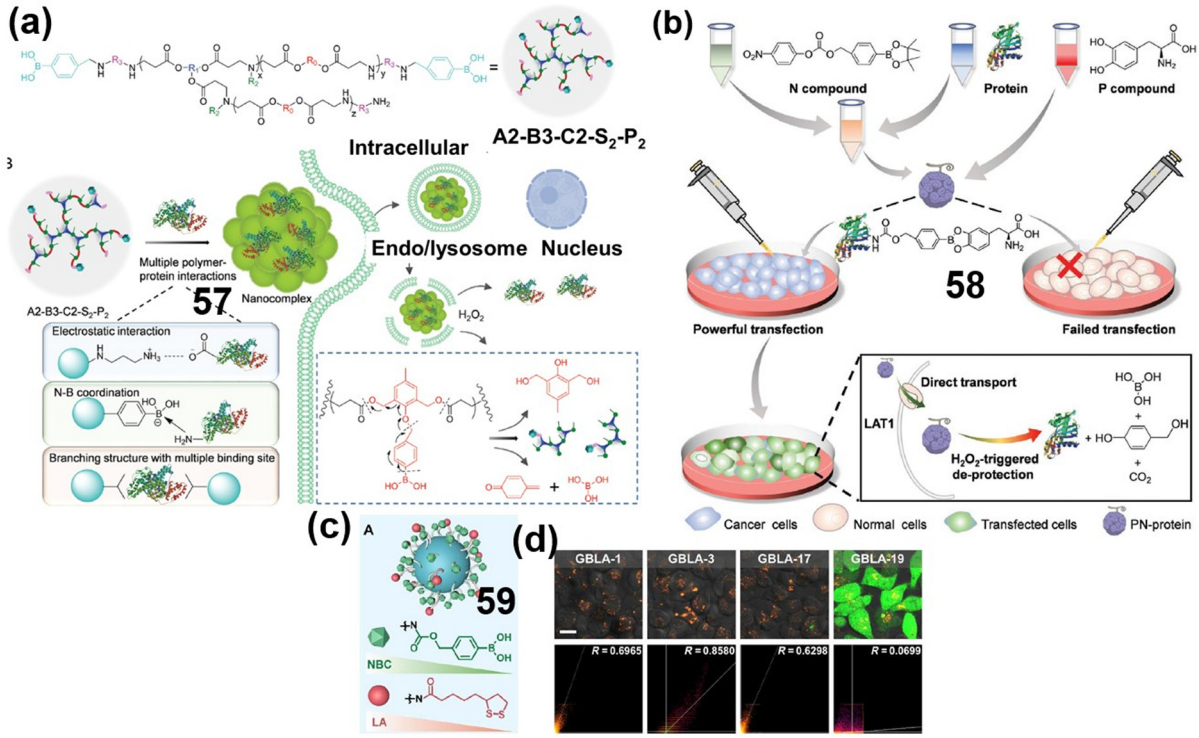

Fig. 15 ROS responsive PBA and PBE agents for tumor targeted delivery of proteins. (a) Chemical constitution of **57** and its working mechanism. Reproduced from ref. 69 with permission from Wiley. (b) Chemical structure and preparation of **58**. Reproduced from ref. 70 with permission from Wiley. (c) Preparation of nano-formulation **59**. (d) Confocal images of HeLa cells treated with the complexes for 4 hours. Reproduced from ref. 71 with permission from Science Advances, copyright © 2025.

efficient cellular uptake. Within tumor cells, the acidic endolysosomal pH and elevated intracellular ROS levels triggered cleavage of the boronate ester bonds, releasing native proteins directly into the cytosol. This system enabled broad-spectrum protein delivery, including enzyme, antibody, and CRISPR-Cas9 ribonucleoprotein complexes, with demonstrated efficacy against the fusion oncogene EWSR1-FLI1 in Ewing sarcoma.

Chen *et al.* (2022) synthesized branched poly(β-amino ester) (PBAE) carriers embedded with pendant PBA units and terminal arginine groups **56** to deliver a wide range of proteins (12–430 kDa) into cancer cells (Fig. 14b).[68] Stable nanocomplexes formed *via* electrostatics, hydrogen bonding, and N–B coordination was rapidly cleaved under tumor-relevant H_2O_2 conditions, leading to cytosolic delivery of saporin and pronounced antitumor efficacy.

Yin *et al.* (2022) designed a hyperbranched PBA-based poly (β-amino ester) (HPAE, **57**, Fig. 15a) that synchronizes strong protein encapsulation with H_2O_2-triggered degradation.[69] By tuning PBA distribution, charge, and branching, this platform achieved efficient cytosolic release of therapeutic proteins including CRISPR-Cas9 RNPs and saporin across diverse isoelectric points and molecular weights. The material preserved bioactivity and selectively released payloads in ROS-rich tumor environments.

Yin *et al.* (2022; Fig. 15b) further introduced a carrier-free pro-protein delivery strategy by covalently modifying proteins with PBE-containing carbonate and LAT1-targeting moieties **58**. These pro-proteins bypassed endosomal entrapment by leveraging LAT1-mediated membrane translocation and underwent selective intracellular activation *via* oxidative PBE cleavage. Saporin pro-proteins injected subcutaneously induced significant tumor regression *in vivo*.[70]

Cheng *et al.* (2024) screened a polymer library functionalized with both lipoic acid and boronate groups, identifying polymer **59** (Table S2.4) as an optimal carrier for cytosolic protein transport (Fig. 15c). ROS-mediated degradation of the dual-ligand scaffold enabled efficient release of monoclonal antibodies, enzymes, and Cas9 RNPs in target tissues. In a psoriasis mouse model, Cas9 delivery *via* **59** successfully disrupted NLRP3 inflammasomes and mitigated inflammation, demonstrating a high therapeutic precision of the delivery.[71]

3.5. Conclusion utilizing PBA and PBE as ROS-responsive materials in personalized medicine

By leveraging the oxidative lability of boronic esters, these exemplified systems has demonstrated selectively to elevated ROS levels, particularly H_2O_2 common in inflamed, ischemic, or cancerous tissues. The studies highlighted in this section demonstrate the breadth of PBA/PBE integration across hydrogels, micelles, prodrugs, and protein delivery systems, enabling site-selective, ROS-triggered drug release with minimal off-target effects.

Mechanistically, these platforms are engineered around H_2O_2-mediated oxidative cleavage of boronic acid or ester groups, leading to network degradation, bond cleavage, or cargo activation. Dual- and multi-responsive designs incorporate secondary triggers such as acidic pH or enzymatic activity, enhancing selectivity and therapeutic control within pathological microenvironments. Many systems are then further functionalized for tissue-specific targeting, offering modular precision in addressing multiple diseases. Importantly, ROS-responsive PBA/PBE constructs minimize systemic toxicity by enabling on-demand degradation and localized therapeutic action. This ensures efficient drug release at sites of pathology while sparing healthy tissue. As with glucose-responsive systems, these materials support feedback-informed and patient-tailored interventions, particularly in diseases where redox balance varies with genetic, metabolic, or environmental factors. In summary, ROS-sensitive PBA and PBE platforms illustrate how biomarker-responsive chemistry can be harnessed to deliver precise, adaptive, and personalized treatments across a spectrum where oxidative stress drive the conditions.

4. Sialic acid-targeting platforms: precision glycobiology in therapy

Glycans –diverse sugar chains attached to proteins and lipids– forms the glycocalyx, a dense molecular interface that coats cell membranes. The glycome, far more structurally complex than the genome or proteome, plays critical roles in cellular communication, immune modulation and barrier function.[72] Sialic acids -Sia- are particularly important due to their terminal positioning on glycoproteins and glycolipids, making them key mediators of both physiological and pathological signaling.[73] In healthy tissues, Sia contribute to self-recognition, protect against proteolytic degradation, and extend the half-life of circulating glycoproteins.[74] They also act as ligands for selectins and Siglecs, regulating leukocyte trafficking and immune tolerance.[75,76] However, especially in cancer, sialylation become dysregulated. Tumors often exhibit hypersialylation, which promotes immune evasion, metastasis, and resistance to therapy.[73] Pathogens similarly exploit sialylation to facilitate host cell entry.[77] Importantly, sialylation profiles differ between individuals, disease stages, and tumor types, making sialoglycans compelling biomarkers for personalized medicine. PBA-functionalized materials can accumulate on cancer cell surfaces, and with appropriate modifications, enable pH-sensitive drug release. Sia features several *cis*-diols, however the C8–C9 positions of its glycerol side chain is spatially accessible, making it an ideal target for PBA-based recognition. Beyond oncology, Sia-targeted platforms show promise in treating central nervous system (CNS) disorders and viral infections, where glycan expression is central to disease progression. In this section, we exemplify PBA-engineered platforms for Sia targeting, highlighting their applications in stratified cancer therapy, glycan-guided drug delivery, and glycobiology-informed immunotherapy.

4.1. Selective targeting of tumor and immune cells *via* glycan signatures

Recent developments include PBA-based nanocarriers and hydrogels that bind Sia overexpressed on cancer cells, enabling localized delivery and minimizing systemic toxicity. Ko *et al.* (2025) presented a novel fluorescent probe **60** (Fig. 16a and Table S3.1), engineered to selectively bind sialylated glycans prevalent on cancer cell surfaces. This specificity enabled precise imaging of tumor tissues, distinguishing them from healthy cells. The probe's design incorporated an oxaborole group, enhancing its binding affinity and fluorescence properties. *In vitro* and *in vivo* evaluations demonstrate SLY (Sialyl Lewis Yellow)'s capability to illuminate cancerous regions with high contrast, facilitating early detection and potentially aiding in surgical planning. This advancement underscores

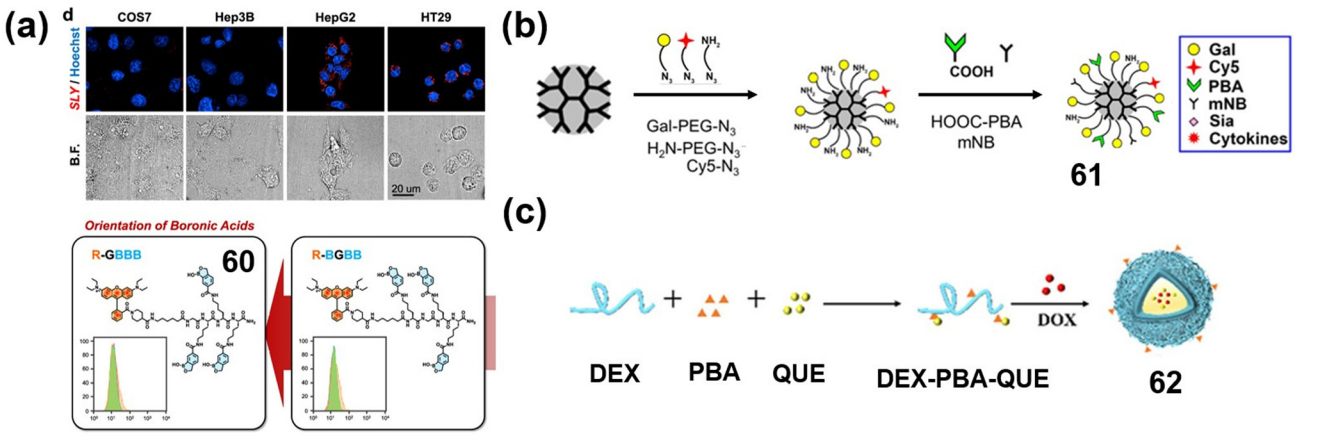

Fig. 16 Self-assembled nanomaterials incorporating PBA units for cell-targeted therapy through specific binding with sialic acid residues. (a) Fluorescence imaging of cell lines using 60 and selected flow cytometry histograms from unbiased library compound screening. Reproduced from ref. 78 with permission from ACS. (b) Structural formulation of 61 and drug loading mechanism. Reproduced from ref. 79 with permission from Wiley. (c) Synthetic procedure for preparing 62. Reproduced from ref. 80 with permission from Elsevier copyright © 2025.

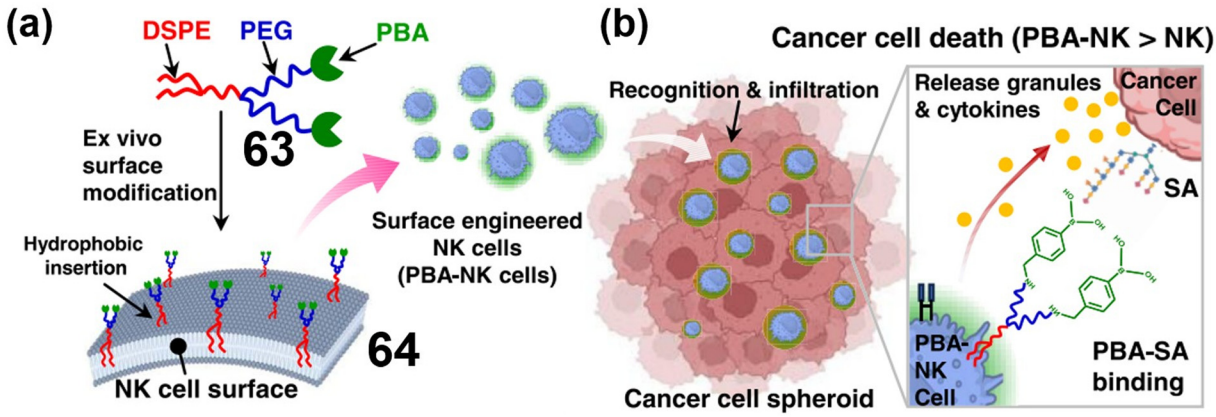

Fig. 17 PBA-functionalized self-assembled nanoparticles designed to bind with sialic acid, thereby enhancing therapeutic efficacy within tumor microenvironments. Graphical illustration of surface-engineered NK cells and utilization for cancer treatment utilizing **63** and **64**. Reproduced from ref. 81 with permission from Elsevier, copyright © 2025.

the growing significance of glycan-targeted imaging agents in cancer diagnostics, offering a promising tool for clinicians to identify malignant tissues more effectively.[78] Chen *et al.* (2024) designed a penta-functional dendritic material (**61**) (Fig. 16b) incorporating PBA, galactose, a Cy5 tag, an amino group, and a photoactivatable mNB moiety. Upon systemic administration and light activation, PBA selectively bound tumor-associated Sia glycans, allowing galactose conjugation *via* photo-cross-linking. This blocked immune-evasive Sia residues and activated immune responses, enhancing tumor cell destruction and offering a novel glycan-guided immunotherapy platform.[79]

To synergize immune activation and chemotherapy, Zhang *et al.* (2024) developed nanocarrier **62** (Fig. 16c), a dextran-based dual-responsive system conjugated with PBA and loaded with DOX and quercetin (QUE). PBA facilitated binding to Sia-overexpressing tumor cells, allowing tumor-specific accumulation. Under acidic and ROS-rich conditions, nanoparticle 43 swelled and triggered co-delivery of DOX (as an immunogenic cell death inducer) and QUE (an anti-inflammatory and immunomodulator). This dual release led to dendritic cell maturation, M1 macrophage polarization, reduced regulatory T-cell infiltration, and enhanced $CD8^+$ T cell activation in melanoma models. The combinatorial responsiveness ensured context-specific activation.[80]

Kim *et al.* (2023) developed PBA–lipid conjugates (**63** and **64**, Fig. 17) that were anchored onto the surface of natural killer (NK) cells *via* PEG linkers. These modified NK cells retained their native immune functionality and showed enhanced cytotoxicity against Sia-overexpressing cancer cells. Targeting was mediated by PBA-Sia interactions, enabling receptor-specific immune cell engagement and efficient recognition of tumor spheroids in both 2D and 3D models.[81]

4.2. Minimized systemic exposure and enhanced localized efficacy

By integrating enzymatically sensitive or pH-responsive drug release mechanisms, Sia targeting systems further improve selectivity and therapeutic impact. Zhang *et al.* (2023) synthesized an enzyme-activatable supramolecular material **65** (Fig. 18a and Table S3.2) by linking PBA and a DDDEEK biomineralization peptide through a phosphorylated tyrosine (pY) domain. In osteosarcoma cells, which overexpress alkaline phosphatase (ALP), dephosphorylation triggered self-assembly and hydrogel coating formation. Selective targeting was achieved *via* PBA binding to Sia-rich tumor glycans, while ALP-induced biomineralization promoted apoptosis to improve efficacy.[82]

Li *et al.* (2022) created amphiphilic polymeric micelles **66** (Fig. 18b) by conjugating a Sia-responsive PBA, Pluronic F127, and ethanolamine to poly(maleic anhydride) through a one-step process. These micelles encapsulated doxorubicin and exhibited pH-sensitive, Sia-dependent release. By varying polymer ratios, Li *et al.* tuned the release rate and tumor selectivity, showing enhanced uptake in Sia-rich HepG2 hepatocellular carcinoma cells. Systemic toxicity was minimized through targeting and localized drug accumulation.[83]

Kim *et al.* (2024) developed PBA-functionalized HA polymersomes **67–68** (Fig. 19a and Table S3.2) for targeted delivery of piperlongumine (PL) to pancreatic tumors. By linking hyaluronic acid (HA) to DSPE-PEG-NH_2 and surface-functionalizing with PBA, these dual-targeted vesicles responded to both HA-CD44 and PBA-Sia interactions. PL was released in a pH-sensitive manner within MIA PaCa-2 pancreatic cancer cells, which overexpressed both CD44 and Sia. Selective glycan recognition enabled preferential uptake over normal pancreatic cells, thereby minimizing off-target effects.[84]

Tian *et al.* (2022) designed mucoadhesive nanomicelles **69** (Fig. 19b) by grafting PBA onto a chitosan oligosaccharide–vitamin E copolymer (PBA-CS-VE) for ocular delivery of voriconazole (VRC). PBA moieties bound covalently to Sia residues on mucins, enhancing mucoadhesion and transcorneal permeability. The system promoted localized retention and controlled drug release, while chitosan transiently disrupted tight

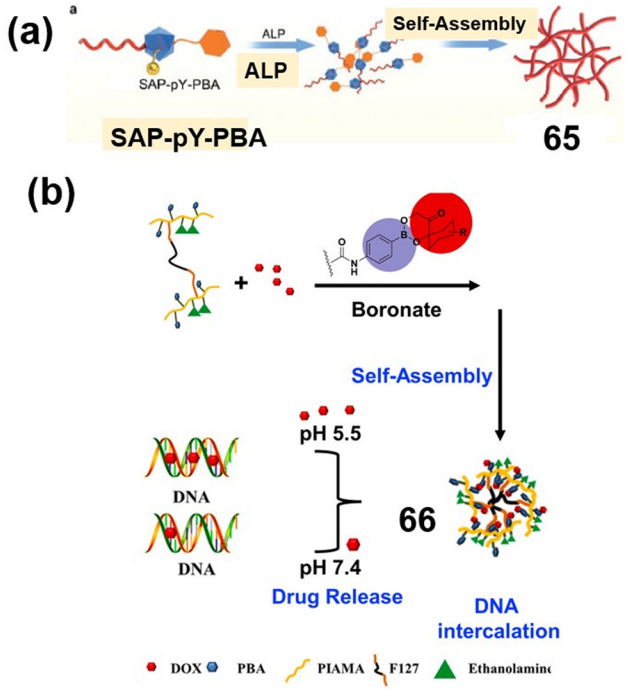

Fig. 18 PBA-functionalized self-assembled nanoparticles capable of reducing systemic exposure while enhancing localized therapeutic efficacy. (a) Self-assembly based formation of **65**. Reproduced from ref. 82 with permission from Wiley. (b) Dynamic crosslinking mechanism for preparing **66** and its biological application. Reproduced from ref. 83 with permission from Elsevier, copyright © 2025.

junctions to facilitate penetration.[85] Hu *et al.* (2024) synthesized a PBA-functionalized injectable copolypeptide hydrogel **70** (Fig. 19c and Table S3.2) *via* ring-opening polymerization of BCys and MGlu *N*-carboxyanhydride monomers. The hydrogel leveraged π–π stacking, N–B coordination, and hydrophobic interactions to encapsulate doxorubicin and its copper complex (**70**), and exhibited multi-stimuli-responsive behavior to Sia, glutathione (GSH), H_2O_2, and acidic pH. Targeting of Sia enhanced tumor accumulation, while injectability and local gelation (5.6–30.3 °C) was used to ensure precise *in situ* drug release.[86]

4.3. Sialylation as a versatile biomarker beyond tumor targeting

While aberrant sialylation is a well-established hallmark of cancer, it also plays a central role in numerous non-cancerous diseases, including viral infections, CNS disorders, atherosclerosis, and cardiovascular diseases (CVDs). In the mammalian CNS, Sia are abundantly expressed, constituting approximately 65% of gangliosides, 32% of glycoproteins, and 3% as free Sia. These levels are tightly regulated, with fluctuations often driven by the translocation of neuraminidases (NEU1/NEU4) to the cell surface. Disruptions in this balance have been linked to neurodegenerative and inflammatory CNS disorders such as Alzheimer's disease, multiple sclerosis, prion diseases, and acute nervous system injury.[87] Beyond the CNS, Sia plays a pivotal role in viral pathogenesis; its recognition by

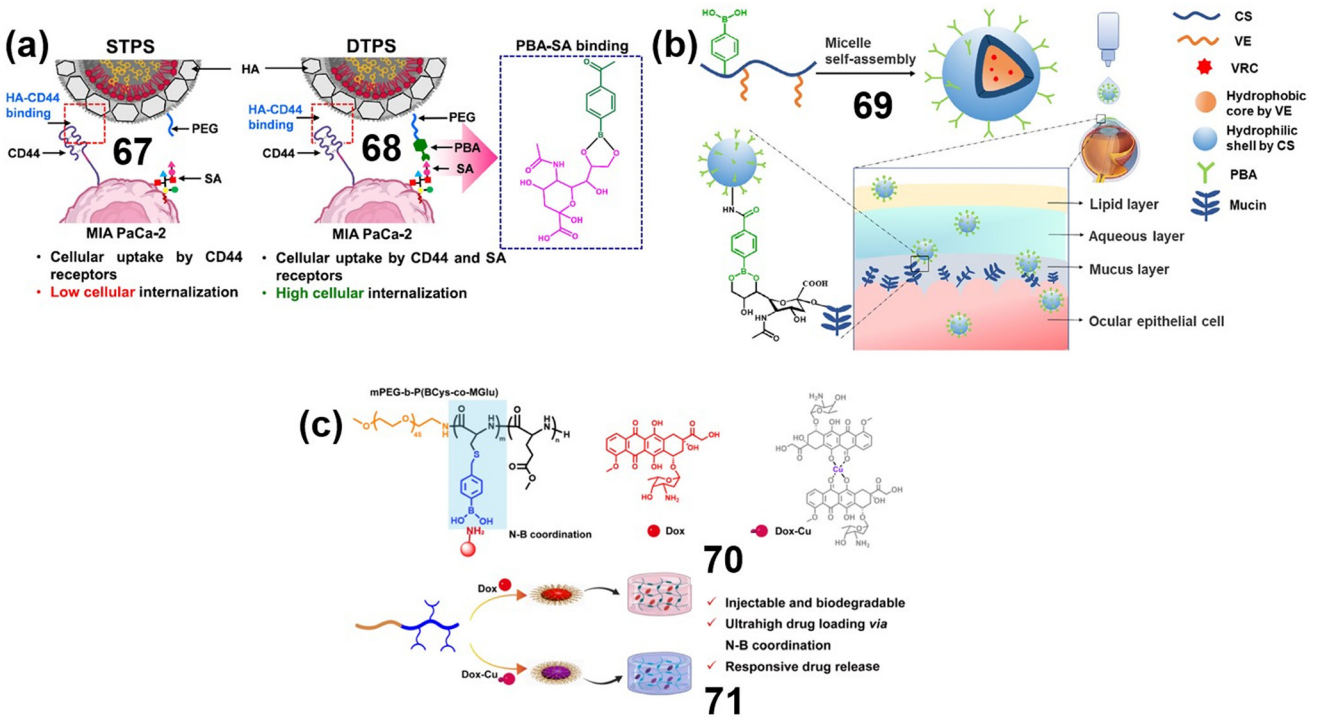

Fig. 19 Self-assembled nanoparticles incorporating PBA molecules to bind with sialic acid, thereby enhancing cellular internalization and improving oncological therapeutic outcomes. (a) Structural components in **67** and **68**. Reproduced from ref. 84 with the permission from Elsevier. (b) Preparation and application of the mucoadhesion nano micelle **69**. Reproduced from ref. 85 with permission from Elsevier. (c) Preparation of PBA functionalized copolypeptides **70** and **71**. Reproduced from ref. 86 with permission from ACS, copyright © 2025.

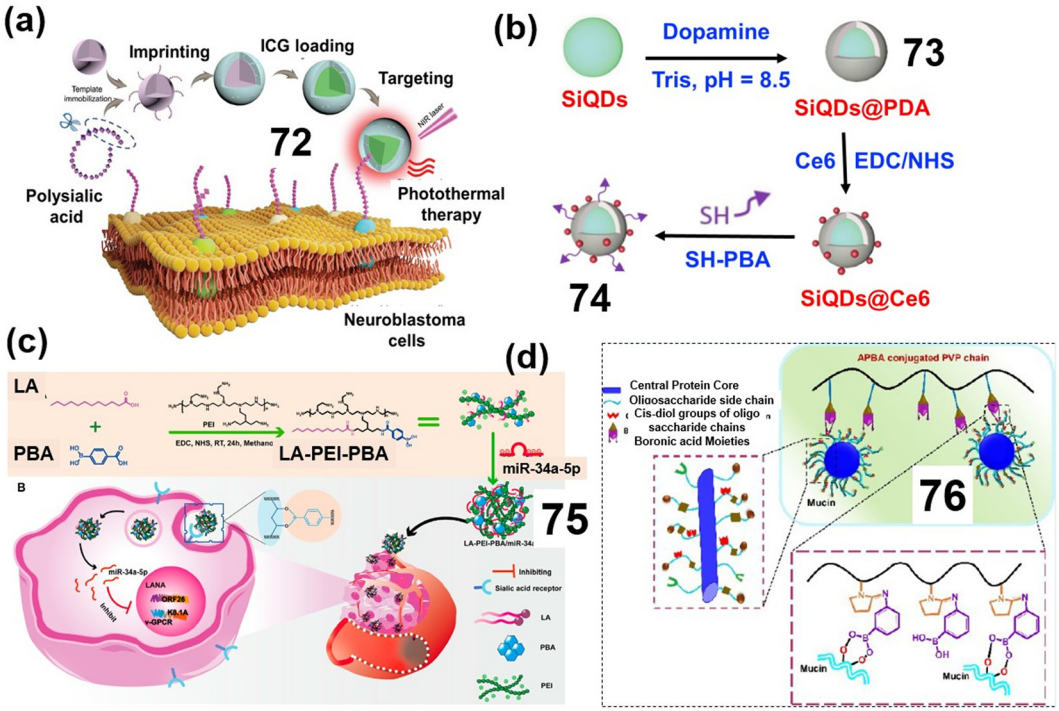

Fig. 20 PBA-based nanomaterials for the detection and binding of sialic acids, enabling diverse therapeutic strategies in cancer treatment. (a) Schematic illustration of preparing nanomaterial **72** and its functioning in photothermal therapeutics. Reproduced from ref. 89 with permission from Wiley (b) Self-assembly based formation of **73** and **74**. Reproduced from ref. 90 with permission from Wiley. (c) Structural formulation and application of **75**. Reproduced from ref. 91 with permission from Frontiers. (d) Constituents of mucoadhesive drug delivery system **76**. Reproduced from ref. 92 with permission ACS, copyright © 2024.

viral surface proteins enables attachment, entry, and replication of viruses such as influenza and coronaviruses. Similarly, in CVDs, altered sialylation profiles—marked by reduced systemic Sia and elevated LDL levels—correlate with disease severity.[87] Due to its widespread involvement in disease processes and its cell-surface accessibility, sialylation presents an adaptable biochemical signature for targeted delivery platforms.[88]

Liu *et al.* (2022) demonstrated that PBA-functionalized silica nanoparticles **72** (Fig. 20a and Table S43.3) could be templated with oligo-Sia chains to form highly specific poly-Sia-recognition sites.[89] By encapsulating near-infrared dyes, this system enabled selective accumulation and photothermal therapy (PTT) in neuroblastoma. Yue *et al.* (2023) further advanced this approach by incorporating PBA into silicon quantum dots **73** (Fig. 20b) alongside the photosensitizer Ce6. The resulting hybrid nanomaterial **74** exhibited dual photothermal and photodynamic therapy (PTT/PDT) effects and preferential tumor accumulation *via* Sia binding. This resulted in ROS production and mitochondrial disruption under laser irradiation, showing promise for CNS malignancies and metastatic disease.[90]

Cui *et al.* (2023) applied PBA chemistry to tackle Kaposi's sarcoma-associated herpesvirus (KSHV) in KSVH-driven CNS pathologies. Their PEI-based nanocarrier **75** (Fig. 20c and Table S4.3) grafted with PBA and lauric acid, electrostatically encapsulated miR-34a-5p, improving its serum stability and targeted delivery. Enhanced uptake in infected endothelial and neural cells led to suppression of both lytic and latent KSHV genes.[91]

Ramesh *et al.* (2024) focused on mucosal drug delivery, developing PBA-modified polyvinylpyrrolidone **76** (Fig. 20d) that bound to Sia residues in mucin. This enhanced mucoadhesion enabled prolonged delivery of propranolol hydrochloride, a beta-blocker used in CVDs. By facilitating stronger tissue binding in the buccal cavity, this system supported sustained therapeutic delivery needed in cardiovascular and systemic disease management.[92]

4.4. Summary utilizing PBA to target sialylation for precision therapy

PBA-functionalized delivery systems have been shown to selectively bind disease-associated Sia for targeted drug delivery, real-time diagnostics, and immune modulation, all essential components of personalized therapeutic strategies. Within pathological microenvironments, sialylation patterns shift dynamically during disease progression. These changes can serve as predictive biomarkers, guiding treatment decisions and enabling non-invasive monitoring of therapeutic efficacy. By integrating Sia expression profiling with PBA-based platforms, clinicians could assess patient responses in real time, reducing reliance on invasive procedures and improving clini-

cal outcomes. In future clinical applications, Sia profiling could inform companion diagnostics and patient eligibility, ensuring that therapies are matched to individual glycan signatures.

5. Conclusion and future outlook

PBA and PBE-functionalized materials represent a versatile class of materials that can be used to design smart, biomarker-responsive platforms for personalized medicine, moving beyond the one-strategy-fits-all-approach. Their ability to form reversible covalent bonds with *cis*-diols enables selective interactions with key physiological markers such as glucose, ROS, pH, and Sia—all of which are tightly linked to disease heterogeneity and patient-specific pathology.

By engineering material responsiveness to these molecular cues, several researchers have developed systems capable of closed-loop therapeutic feedback, where real-time disease signals directly trigger therapeutic actions. This includes insulin release in response to glucose fluctuations in diabetes, targeted cancer cell death *via* ROS-amplification, and tumor-selective drug delivery *via* Sia recognition. Such systems are not only responsive and adaptive, but also increasingly modular, allowing integration of multiple stimuli—such as pH and enzymatic activity—for precision control in complex biological microenvironments.

Beyond therapeutic delivery, PBA/PBE chemistries hold great promise in diagnostics and digital health. Their incorporation into biosensors and wearable devices could enable real-time monitoring of fluctuating biomarkers like glucose or oxidative stress, facilitating feedback-directed dosing and early clinical intervention. The convergence of chemical responsiveness with digital interfaces opens the door to highly personalized disease management systems.

While boron-containing compounds were once considered toxic, this view has evolved. Boron is now regarded as generally safe for medicinal use, and its abundance in nature makes it an attractive component for drug development.[93] Although PBA itself is not an FDA-approved drug, it serves as a key building block in several approved therapeutics, including bortezomib (Velcade®),[94] ixazomib (Ninlaro®) and vaborbactam (Vabomere ®). These drugs are used to treat conditions such as multiple myeloma and complicated urinary tract infections. PBA is also used as an excipient in some formulations, with its safety profile well documented through FDA review. Yet, despite its widespread use in preclinical systems, no PBA-based biomaterial has yet received FDA approval as a standalone therapeutic. Most development remain at the proof-of-concept or preclinical stage, with challenges such as physiological stability, off-target binding, and regulatory hurdles limiting clinical translation.

To realize their potential, several major challenges must be addressed. A major concern is off-target binding, particularly with endogenous diols, which can compromise both specificity and safety. This issue is evident in studies discussed sections 2 and 4, where 3-amino-, and 3-fluorinated PBAs have been employed to target either glucose or Sia. Both monosaccharides possess vicinal 1,2-diol motifs but differ in stereochemistry and molecular context. Sia features a highly accessible and reactive diol at the C8 and C9 positions of its glycerol side chain, while glucose's rigid pyranose ring and *trans*-oriented hydroxyls reduce reactivity due to steric hindrance. Sia is typically targeted in its glycan-incorporated form, where its exposed *cis*-diol motif facilitates selective recognition. Careful scaffold design is essential to ensure preferential binding to Sia over glucose. Strategies to improve specificity include chemical tuning of boronic acid groups, multivalent interactions targeting the α-hydroxy-carboxylic acid moiety, or molecular imprinting and polymer architecture optimization.

In the future, the full potential of PBA/PBE systems lies in their ability to integrate patient stratification data– including genomic, proteomic, and metabolomic profiles– into material design. This data-driven personalization could enable therapeutic systems that are finely tuned to a patient's unique biomolecular landscape or individualized material responses, ensuring that therapeutic systems are precisely aligned with a patient's unique biomolecular landscape.

In summary, PBA and PBE-based materials exemplify the next generation of smart biomaterials—platforms capable of sensing, responding, and adapting to the dynamic needs of individual patients. Their dual utility in diagnostics and therapy, multi-stimuli responsiveness, and potential for digital integration, makes them strong candidates for advancing real-time, precision-guided healthcare. To fulfill this promise, interdisciplinary collaboration will be essential to refine their safety, specificity, and scalability.

Author contributions

Ratish R. Nair: writing – review & editing, writing – original draft, visualization, methodology, data curation. Loise Råberg: editing, figure preparation, visualization. Hanna Mårtensson: editing, figure preparation, visualization. Fanny Jia: editing, figure preparation. Yifan Gu: editing, figure preparation. Gizem Erensoy: discussions, visualization, Hamza Yakubu: editing. Alexandra Stubelius: writing – review & editing, supervision, visualization, methodology, project administration, funding acquisition, conceptualization, data curation.

Conflicts of interest

There are no conflicts to declare.

Data availability

No primary research results, software or code have been included, and no new data were generated or analyzed as part of this review.

Supplementary information (SI) is available, containing information regarding mentioned platforms, stimulus, mechanism of responsiveness, clinical target, and personalization feature. See DOI: https://doi.org/10.1039/d5bm01624j.

Acknowledgements

This work was supported by Chalmers Technical University and its Area of Advance Nano. The authors greatly acknowledge further financial support from the Carl Tryggers Foundation (CTS23-2730), Apotekare Hedbergs Stiftelse för Medicinsk Forskning, the Swedish Research Council (2021-01870), the Swedish Rheumatism Association (R-981253), the King Gustav V's 80 years' foundation (FAI-2022-0872) and IngaBritt och Arne Lundbergs Forskningsstiftelse (LU2022-0041). This study was accomplished within the context of the National ATMP Research School funded by the Swedish Research Council.

References

1 J. J. Lavigne, *J. Am. Chem. Soc.*, 2006, **128**, 13969–13970.
2 J. P. M. António, R. Russo, C. P. Carvalho, P. M. S. D. Cal and P. M. P. Gois, *Chem. Soc. Rev.*, 2019, **48**, 3513–3536.
3 P. J. Duggan, *Aust. J. Chem.*, 2004, **57**, 291–299.
4 G. Fang, H. Wang, Z. Bian, J. Sun, A. Liu, H. Fang, B. Liu, Q. Yao and Z. Wu, *RSC Adv.*, 2018, **8**, 29400–29427.
5 Z. Bian, A. Liu, Y. Li, G. Fang, Q. Yao, G. Zhang and Z. Wu, *Analyst*, 2020, **145**, 719–744.
6 R. R. Nair, S. Debnath, S. Das, P. Wakchaure, B. Ganguly and P. B. Chatterjee, *ACS Appl. Bio Mater.*, 2019, **2**, 2374–2387.
7 P. R. Westmark and B. D. Smith, *J. Am. Chem. Soc.*, 1994, **116**, 9343–9344.
8 M. Ji, P. Li, N. Sheng, L. Liu, H. Pan, C. Wang, L. Cai and Y. Ma, *ACS Appl. Mater. Interfaces*, 2016, **8**, 9565–9576.
9 Y. Xiong, M. Li, Q. Lu, G. Qing and T. Sun, *Polymers*, 2017, **9**, 249.
10 W. Chen, W. Xie, G. Zhao and Q. Shuai, *Molecules*, 2023, **28**, 4461.
11 B. C. Das, P. Chokkalingam, P. Masilamani, S. Shukla and S. Das, *Int. J. Mol. Sci.*, 2023, **24**, 2757.
12 A. Stubelius, S. Lee and A. Almutairi, *Acc. Chem. Res.*, 2019, **52**, 3108–3119.
13 C. Achilli, A. Ciana, M. Fagnoni, C. Balduini and G. Minetti, *Cent. Eur. J. Chem.*, 2013, **11**, 137–139.
14 W. L. A. Brooks, C. C. Deng and B. S. Sumerlin, *ACS Omega*, 2018, **3**, 17863–17870.
15 W. Zhai, X. Sun, T. D. James and J. S. Fossey, *Chem. – Asian J.*, 2015, **10**, 1836–1848.
16 J. P. Lorand and J. O. Edwards, *J. Org. Chem.*, 1959, **24**, 769–774.
17 M. K. Ediriweera and S. Jayasena, *Metabolites*, 2023, **13**, 345.
18 Y. Yao, K. Ji, Y. Wang, Z. Gu and J. Wang, *Acc. Mater. Res.*, 2022, **3**, 960–970.
19 D. R. Matthews, A. S. Rudenski, M. A. Burnett, P. Darling and R. C. Turner, *Clin. Endocrinol.*, 1985, **23**, 71–79.
20 L. Rosenfeld, *Clin. Chem.*, 2002, **48**, 2270–2288.
21 S. Chen, T. Miyazaki, M. Itoh, H. Matsumoto, Y. Moro-Oka, M. Tanaka, Y. Miyahara, T. Suganami and A. Matsumoto, *Gels*, 2022, **8**, 74.
22 W. J. Kim, Y.-J. Kwon, C.-H. Cho, S.-K. Ye and K. O. Kim, *Sci. Rep.*, 2021, **11**, 21894.
23 Y. Wang, P. Chen, W. Liu, X. Wei, J. Zhang, X. Wei, Y. Liu, L. Rao, S. Zhang, J. Yu, X. Ye, J. Wang and Z. Gu, *Nano Today*, 2023, **51**, 101937.
24 K. Ji, X. Wei, A. R. Kahkoska, J. Zhang, Y. Zhang, J. Xu, X. Wei, W. Liu, Y. Wang, Y. Yao, X. Huang, S. Mei, Y. Liu, S. Wang, Z. Zhao, Z. Lu, J. You, G. Xu, Y. Shen, J. B. Buse, J. Wang and Z. Gu, *Nat. Nanotechnol.*, 2024, **19**, 1880–1891.
25 M. A. VandenBerg, S. Xian, Y. Xiang and M. J. Webber, *Macromol. Biosci.*, 2024, **24**, 2300001.
26 Y. Liu, Y. Wang, Y. Yao, J. Zhang, W. Liu, K. Ji, X. Wei, Y. Wang, X. Liu, S. Zhang, J. Wang and Z. Gu, *Angew. Chem., Int. Ed.*, 2023, **62**, e202303097.
27 M. Patil, N. J. Deshmukh, M. Patel and G. V. Sangle, *Peptides*, 2020, **127**, 170296.
28 S. Yu, Z. Ye, R. Roy, R. R. Sonani, I. Pramudya, S. Xian, Y. Xiang, G. Liu, B. Flores, E. Nativ-Roth, R. Bitton, E. H. Egelman and M. J. Webber, *Adv. Mater.*, 2024, **36**, 2311498.
29 D. Vinciguerra, P. S. Rajalakshmi, J. Yang, P. G. Georgiou, K. Snell, T. Pesenti, J. Collins, M. Tamboline, S. Xu, R. M. van Dam, K. M. M. Messina, A. L. Hevener and H. D. Maynard, *ACS Cent. Sci.*, 2024, **10**, 2036–2047.
30 W. Chen, S. Yu, B. Webber, E. L. DeWolf, R. Kilmer, S. Xian, C. R. Schmidt, E. M. Power and M. J. Webber, *J. Biomed. Mater. Res., Part A*, 2025, **113**, e37854.
31 D. Shen, H. Yu, L. Wang, J. Feng, Q. Zhang, J. Pan, Y. Han, Z. Ni, R. Liang and M. A. Uddin, *J. Controlled Release*, 2022, **352**, 527–539.
32 S. Saha, A. Ali, S. Saroj, D. Jinagal, T. Rakshit and S. Pal, *Chem. – Asian J.*, 2024, **19**, e202400873.
33 K. Yang, H. Bo, D. Ma, M. Peng, Q. Liu, Z. Heng, Z. Gu, X. Liu and S. Chen, *Soft Matter*, 2024, **20**, 8855–8865.
34 R. Ying, W. Wang, R. Chen, R. Zhou and X. Mao, *Biomacromolecules*, 2024, **25**, 7446–7458.
35 M. Li, N. Wang, R. Liu, X. Zhang, W. He, W. Zhang, J. Li, C. Peng and Y. Li, *Theranostics*, 2024, **14**, 5596–5607.
36 J. Chen, Y. Guo, Y. Zheng, Z. Chen, H. Xu, S. Pan, X. Liang, L. Zhai and Y.-Q. Guan, *J. Colloid Interface Sci.*, 2025, **684**, 769–782.
37 Y. Y. Jiang, J. C. Shui, B. X. Zhang, J. W. Chin and R. S. Yue, *Front. Pharmacol.*, 2020, **11**, 585487.
38 Z. Xu, G. Liu, J. Huang and J. Wu, *ACS Appl. Mater. Interfaces*, 2022, **14**, 7680–7689.
39 Z. Xu, G. Liu, P. Liu, Y. Hu, Y. Chen, Y. Fang, G. Sun, H. Huang and J. Wu, *Acta Biomater.*, 2022, **147**, 147–157.

40 Y. Liang, M. Li, Y. Yang, L. Qiao, H. Xu and B. Guo, *ACS Nano*, 2022, **16**, 3194–3207.
41 W. Zhang, K. Zha, Y. Xiong, W. Hu, L. Chen, Z. Lin, C. Yu, W. Zhou, F. Cao, H. Hu, B. Mi and G. Liu, *Bioact. Mater.*, 2023, **30**, 29–45.
42 X. Zhang, K. Ren, C. Xiao and X. Chen, *Acta Biomater.*, 2023, **172**, 206–217.
43 Y. Liu, T. Liu, Z. Zhu, L. Xie, D. Bai, T. Liu, W. Gu, W. Li, Y. Shu and J. Zhang, *Acta Biomater.*, 2024, **190**, 79–94.
44 F. He, P. Xu, Z. Zhu, Y. Zhang, C. Cai, Y. Zhang, J. Shao, F. Jin, Q. Li, J. You, H. Zhou, W. Zhang, J. Wei, X. Hong, Z. Zhang, C. Han, Y. Zhang, Z. Gu and X. Wang, *Adv. Healthcare Mater.*, 2024, 2400150.
45 H. Wang, W. You, B. Wu, X. Nie, L. Xia, C. Wang and Y.-Z. You, *J. Mater. Chem. B*, 2022, **10**, 2844–2852.
46 Q. Ma, L. Bian, X. Zhao, X. Tian, H. Yin, Y. Wang, A. Shi and J. Wu, *Mater. Today Bio*, 2022, **13**, 100181.
47 H. Ye, Y. Zhou, X. Liu, Y. Chen, S. Duan, R. Zhu, Y. Liu and L. Yin, *Biomacromolecules*, 2019, **20**, 2441–2463.
48 D. H. Kim, H. S. Hwang and K. Na, *Biomacromolecules*, 2018, **19**, 3301–3310.
49 M. Pu, H. Cao, H. Zhang, T. Wang, Y. Li, S. Xiao and Z. Gu, *Mater. Horiz.*, 2024, **11**, 3721–3746.
50 S. Lee, A. Stubelius, N. Hamelmann, V. Tran and A. Almutairi, *ACS Appl. Mater. Interfaces*, 2018, **10**, 40378–40387.
51 X. Yao, W. Sun, Y. Yuan, J. Hu, J. Fu and J. Yin, *Bioorg. Chem.*, 2024, **150**, 107560.
52 T. Hao, M. Qian, Y. Zhang, Q. Liu, A. C. Midgley, Y. Liu, Y. Che, J. Hou and Q. Zhao, *Adv. Sci.*, 2022, **9**, 2105408.
53 S. Wang, Y. Yao, T. Zhou, J. Xie, J. Ding, W. Cao, L. Shen, Y. Zhu and C. Gao, *Composites, Part B*, 2022, **238**, 109941.
54 F. Jia, B. Yu, J. Li, F. Cai, G. Fu, Q. Jin and J. Ji, *Adv. Healthcare Mater.*, 2023, **12**, 2301615.
55 F. Dai, F. Chen, J. Zhang, X. Chen, H. Liang, Z. Liang, S. Zhang, H. Tan and L. Zhao, *ACS Appl. Nano Mater.*, 2024, **7**, 7289–7299.
56 W. Lin, K. Hu, C. Li, W. Pu, X. Yan, H. Chen, H. Hu, H. Deng and J. Zhang, *Adv. Mater.*, 2022, **34**, 2204455.
57 X. Zhang, Y. Sun, R. Yang, B. Liu, Y. Liu, J. Yang and W. Liu, *Biomaterials*, 2022, **287**, 121656.
58 X. Zhou, X. Ning, Y. Chen, H. Chang, D. Lu, D. Pei, Z. Geng, Z. Zeng, C. Guo, J. Huang, S. Yu and H. Guo, *ACS Mater. Lett.*, 2023, **5**, 3142–3155.
59 X. Gao, C. Yuan, E. Tan, Z. Li, Y. Cheng, J. Xiao and G. Rong, *J. Controlled Release*, 2023, **355**, 675–684.
60 Q. Wang, Z. Dong, F. Lou, Y. Yin, J. Zhang, H. Wen, T. Lu and Y. Wang, *Drug Delivery*, 2022, **29**, 2029–2043.
61 F. Shuai, Y. Yin, Y. Yao, L. Deng, Y. Wen, H. Zhao and X. Han, *Biomaterials*, 2025, **316**, 123024.
62 M. Wang, Q. Hu, J. Huang, F. Zhang, Z. Yao, S. Shao, X. Zhao and T. Liang, *Adv. Healthcare Mater.*, 2023, **12**, 2203264.
63 D. Bi, F. Qu, W. Xiao, J. Wu, P. Liu, H. Du, Y. Xie, H. Liu, L. Zhang, J. Tao, Y. Liu and J. Zhu, *ACS Nano*, 2023, **17**, 4346–4357.
64 Q. Wang, K. Feng, G. Wan, W. Liao, J. Jin, P. Wang, X. Sun, W. Wang and Q. Jiang, *J. Nanobiotechnol.*, 2025, **23**, 18.
65 Q. Yang, N. Liu, Z. Zhao, X. Liu and L. Yin, *Nano Res.*, 2024, **17**, 1760–1771.
66 J. Lv, Z. Yang, C. Wang, J. Duan, L. Ren, G. Rong, Q. Feng, Y. Li and Y. Cheng, *J. Controlled Release*, 2023, **355**, 160–170.
67 X. Liu, Z. Zhao, W. Li, Y. Li, Q. Yang, N. Liu, Y. Chen and L. Yin, *Angew. Chem., Int. Ed.*, 2023, **62**, e202307664.
68 R. Lu, Y. Zheng, M. Wang, J. Lin, Z. Zhao, L. Chen, J. Zhang, X. Liu, L. Yin and Y. Chen, *Acta Biomater.*, 2022, **152**, 355–366.
69 X. Liu, Z. Zhao, F. Wu, Y. Chen and L. Yin, *Adv. Mater.*, 2022, **34**, 2108116.
70 Z. Zhao, X. Liu, M. Hou, R. Zhou, F. Wu, J. Yan, W. Li, Y. Zheng, Q. Zhong, Y. Chen and L. Yin, *Adv. Mater.*, 2022, **34**, 2110560.
71 E. Tan, T. Wan, Q. Pan, J. Duan, S. Zhang, R. Wang, P. Gao, J. Lv, H. Wang, D. Li, Y. Ping and Y. Cheng, *Sci. Adv.*, 2024, **10**, eadl4336.
72 S. Weinbaum, J. M. Tarbell and E. R. Damiano, *Annu. Rev. Biomed. Eng.*, 2007, **9**, 121–167.
73 R. Schauer and J. P. Kamerling, *Adv. Carbohydr. Chem. Biochem.*, 2018, **75**, 1–213.
74 A. G. Morell, G. Gregoriadis, I. H. Scheinberg, J. Hickman and G. Ashwell, *J. Biol. Chem.*, 1971, **246**, 1461–1467.
75 P. Göröug and J. D. Pearson, *J. Pathol.*, 1985, **146**, 205–212.
76 M. S. Macauley, P. R. Crocker and J. C. Paulson, *Nat. Rev. Immunol.*, 2014, **14**, 653–666.
77 J. E. Stencel-Baerenwald, K. Reiss, D. M. Reiter, T. Stehle and T. S. Dermody, *Nat. Rev. Microbiol.*, 2014, **12**, 739–749.
78 K. Ko, M. Gao, S. Sarkar, H.-Y. Kwon and Y.-T. Chang, *J. Am. Chem. Soc.*, 2025, **147**, 19718–19726.
79 Y. Yang, Y. Li, C. Wang, Y. Wang, Y. Ren, J. Wu, H. Ju and Y. Chen, *Angew. Chem., Int. Ed.*, 2024, **63**, e202319849.
80 L. Wang, S. He, R. Liu, Y. Xue, Y. Quan, R. Shi, X. Yang, Q. Lin, X. Sun, Z. Zhang and L. Zhang, *Acta Pharm. Sin. B*, 2024, **14**, 2263–2280.
81 A. K. Jangid, S. Kim, H. W. Park, H. J. Kim and K. Kim, *Biomacromolecules*, 2024, **25**, 222–237.
82 X. Yang, S. Gao, B. Yang, Z. Yang, F. Lou, P. Huang, P. Zhao, J. Guo, H. Fang, B. Chu, M. He, N. Wang, A. H. L. Chan, R. H. F. Chan, Z. Wang, L. Bian and K. Zhang, *Adv. Sci.*, 2023, **10**, 2302272.
83 R. Feng, L. Zhu, F. Teng, M. Wang, S. Chen, Z. Song and H. Li, *Colloids Surf., B*, 2022, **216**, 112559.
84 A. K. Jangid, S. Kim and K. Kim, *Int. J. Biol. Macromol.*, 2024, **275**, 133738.
85 X. Sun, Y. Sheng, K. Li, S. Sai, J. Feng, Y. Li, J. Zhang, J. Han and B. Tian, *Acta Biomater.*, 2022, **138**, 193–207.
86 R. Wang, B. Yin, Y. Guo, X. Wu, F. Lv, X. Qu and X. Hu, *ACS Appl. Polym. Mater.*, 2024, **6**, 11653–11663.
87 W. Zhu, Y. Zhou, L. Guo and S. Feng, *Cell Death Discovery*, 2024, **10**, 415.
88 A. Ruelland, G. Gallou, B. Legras, F. Paillard and L. Cloarec, *Clin. Chim. Acta*, 1993, **221**, 127–133.

89 S. Xu, M. Zhao, Z. Gu, H. Lu and Z. Liu, *Small*, 2022, **18**, 2201671.
90 F. Liu, J. Lin, Y. Luo, D. Xie, J. Bian, X. Liu and J. Yue, *Biomater. Sci.*, 2023, **11**, 4009–4021.
91 F. Li, D. Cao, L. Yao, W. Gu, Z. Liu, D. Li and L. Cui, *Front. Bioeng. Biotechnol.*, 2023, **11**, 1343956.
92 M. Surendranath, R. M. Ramesan, P. Nair and R. Parameswaran, *ACS Appl. Bio Mater.*, 2024, **7**, 7429–7443.
93 J. Plescia and N. Moitessier, *Eur. J. Med. Chem.*, 2020, **195**, 112270.
94 R. C. Kane, A. T. Farrell, R. Sridhara and R. Pazdur, *Clin. Cancer Res.*, 2006, **12**, 2955–2960.